TITLE:

Flow field control to mitigate airborne sea salt adhesion on bridge girders

AUTHOR(S):

Mbithi, Michael; Yagi, Tomomi; Noguchi, Kyohei; Shigeta, Masatoshi; Sugii, Kenichi; Shirato, Hiromichi

CITATION:

Mbithi, Michael ...[et al]. Flow field control to mitigate airborne sea salt adhesion on bridge girders. Structure and Infrastructure Engineering 2018, 14(3): 348-364

ISSUE DATE:

2018

URL:

http://hdl.handle.net/2433/276815

RIGHT:

This is an Accepted Manuscript of an article published by Taylor & Francis in Structure and Infrastructure Engineering on 25 Jul 2017, available at: http://www.tandfonline.com/10.1080/15732479.2017.1354031.; The full-text file will be made open to the public on 25 Jul 2018 in accordance with publisher's 'Terms and Conditions for Self-Archiving'.; This is not the published version. Please cite only the published version. この論文は出版社版でありません。引用の際には出版社版をご確認ご利用ください。

京都大学学術情報リポジトリ
KURENAI 紅
Kyoto University Research Information Repository

京都大学 KYOTO UNIVERSITY
A Self-archived copy in
Kyoto University Research Information Repository
https://repository.kulib.kyoto-u.ac.jp
京都大学学術情報リポジトリ KURENAI 紅 Kyoto University Research Information Repository

Flow field control to mitigate airborne sea salt adhesion on bridge girders

Michael MBITHI[a1], Tomomi YAGI[a*], Kyohei NOGUCHI[a], Masatoshi SHIGETA[a] Kenichi SUGII[b], and Hiromichi SHIRATO[a]

[a]*Department of Civil and Earth Resources Engineering, Kyoto University, Kyoto, 615-840, Japan*

[b]*Hanshin Expressway Engineering Company Limited, Osaka, 550-0005, Japan*

[*]Corresponding author. Email: yagi.tomomi.7a@kyoto-u.ac.jp

Michael MBITHI is a graduate student at Kyoto University. His research interests focus on maintenance of bridge structures especially through reduction of airborne sea salt adhesion amount on bridge girders.

Tomomi YAGI is a professor of Structural Engineering at Kyoto University. His work focuses on wind-induced instabilities of structures, especially the mechanism of wind-induced vibrations of bridges and development of their countermeasures.

Kyohei NOGUCHI is a Ph.D. candidate at Kyoto University. His research interests focus on adhesion of airborne sea salt onto structural members.

Masatoshi SHIGETA is a graduate student at Kyoto University. His research interests focus on countermeasures against corrosion of bridges due to airborne sea salt.

Kenichi SUGII is a professional Structural Engineer involved in design and maintenance of civil infrastructures.

Hiromichi SHIRATO is a professor of Structural Engineering at Kyoto University. His work focuses on experimental and analytical study on mechanism of aerodynamic phenomena for engineering structures.

京都大学 KYOTO UNIVERSITY
A Self-archived copy in
Kyoto University Research Information Repository
https://repository.kulib.kyoto-u.ac.jp
京都大学学術情報リポジトリ KURENAI 紅 Kyoto University Research Information Repository

Flow field control to mitigate airborne sea salt adhesion on bridge girders

In order to realise effective maintenance and enhanced durability of structures, it is important to also reduce corrosion of bridges by airborne sea salt. The objective of this study is to reduce airborne sea salt adhesion amount on steel girder bridges by employing aerodynamic countermeasures. The study bridge is a typical metropolitan highway bridge with 8 I-shaped steel girders located in Japan. Aerodynamic countermeasure devices are employed to change the flow field around the bridge structure in an attempt to reduce wind velocity normal to the bridge girders. Devices existing on urban bridges such as noise barriers, median barriers, and facilities for passage of drainage pipes and electric cables, modelled as horizontal plates, are modified and investigated for their ability to reduce airborne sea salt adhesion amount. As additional devices, vertical plates are installed to change the flow separation and their applicability is also studied. Computational fluid dynamics (CFD) is employed for flow field simulations and airborne sea salt adhesion amount is estimated by the improved concentration flux method. Findings indicate that horizontal plates and vertical plates significantly reduce airborne sea salt adhesion amount. Noise barriers and median barriers can also reduce airborne sea salt adhesion amount.

Keywords: airborne sea salt; aerodynamic countermeasures; concentration flux method; bridge maintenance

Subject classification codes: include these here if the journal requires them

1. Introduction

In many countries worldwide, maintenance of civil infrastructures to achieve longevity is becoming necessary. With the ever-increasing pace of modernisation and the stress it causes particularly to transport infrastructure, longevity and effective maintenance are becoming issues that need to be addressed urgently. In fact, in many developed countries where most infrastructures were constructed decades ago, the main focus now is on achieving effective maintenance of structures due to the problem of aging

京都大学 KYOTO UNIVERSITY
A Self-archived copy in
Kyoto University Research Information Repository
https://repository.kulib.kyoto-u.ac.jp
京都大学学術情報リポジトリ KURENAI 紅 Kyoto University Research Information Repository

deterioration. In the future, developing countries are speculated to experience similar problems. With specific reference to bridge structures, the service life is normally estimated as 50 years and in Japan for example; many bridges were constructed during the rapid economic growth period of the 1960's. In the next decade, most of these bridges will have surpassed the service life and the damage risk due to deterioration of structural members is bound to increase. Concretely, the ratio of bridges past 50 years old to the total number of bridges is approximated to be 67% in 2033 (The Ministry of Land, Infrastructure, Transport and Tourism, [MLIT], 2013). Similarly, in America the Federal Highway Administration (FHWA) classified more than 11% of total highway bridges as structural deficient implying they require significant maintenance, rehabilitation, or replacement. Approximately 33% of all national highway bridges were rated as having exceeded their lifespan and predicted that without substantial replacement, approximately 64% of all bridges will be over 50 years old by 2030. (Transportation for America 2010).

Corrosion of steel can result from several different factors ranging from de-icing salt applied during winter to adhesion of airborne sea salt onto structural members. Corrosion by the latter mainly affects structures located at or near coastal areas. Generally, sea salt particles are transported by the wind and deposited on the surface of bridge girders thus inducing corrosion. The amount of deposited salt is closely related to the progress rate of corrosion. In addition, countries surrounded by the sea such as Japan experience severe corrosion of steel by airborne sea salt and this has a high influence on durability of bridge structures. To realise effective maintenance and enhanced durability of bridge structures, it is therefore crucial to reduce the amount of airborne sea salt adhesion on bridge girders.

京都大学 KYOTO UNIVERSITY
A Self-archived copy in
Kyoto University Research Information Repository
https://repository.kulib.kyoto-u.ac.jp
京都大学学術情報リポジトリ KURENAI 紅 Kyoto University Research Information Repository

Problems related to sea salt particles are diverse and wide-ranging. Corvo, Betancourt, and Mendoza (1995) proposed a model of the influence of chloride and SO_2 deposition rate on atmospheric corrosion of steel. Findings indicated that the influence of chloride ions is significant in determining the corrosion rate of steel when a corrosion products layer is already formed. In the case that the corrosion products layer is not completely formed, the influence of time of wetness is important. Lovett (1978) performed quantitative measurement of airborne sea salt in the North Atlantic and attempted to correlate sea salt concentration with wind speed and other meteorological factors. Manders et al. (2010) provided more insight into the distribution of sea salt across Europe by presenting a compilation of existing data on sodium and using the data to verify calculated sea salt distributions from a chemistry transport model. Chen, Chiu, Chan, Chang, and Yang (2012) proposed a model to predict the distribution of airborne sea salt in the coastal region of Northern Taiwan based on results of airborne sea salt measurement at several sites. Cole, Lau, Chan and Paterson (2013) conducted experimental studies aimed at determining the mechanisms of salt removal from metallic surfaces by wind and rain.

In the case of bridge structures, Obata, Li, Watanabe, and Goto (2014) pursued numerical methods to simulate adhesion of sea salt particles on bridge girders based on local and global approaches. In local analysis, adhesion of sea salt particles was simulated by computational fluid dynamics (CFD) with the Lagrangian type of modelling of airborne sea salt particles. In global analysis, the concentration of airborne sea salt particles was simulated by a meteorological program with a chemistry package. Noguchi et al. (2013, 2015) conducted a study to improve the estimation accuracy of airborne salt adhesion amount on a structural surface based on inertial collision and diffusive motion of sea salt particles. The sea salt adhesion amount on a steel girder

京都大学 KYOTO UNIVERSITY
A Self-archived copy in
Kyoto University Research Information Repository
https://repository.kulib.kyoto-u.ac.jp
京都大学学術情報リポジトリ KURENAI 紅 Kyoto University Research Information Repository

bridge was estimated using meteorologically observed data and results of 3D flow field analysis taking into account the surrounding geography. Washing-out effect due to rain was also applied on the outer surfaces of the most upstream and downstream girders. Noguchi et al. (2014) also discussed the deposition of sea salt onto a structural surface based on the physical behaviour of each sea salt particle using the particle tracing method. Chendra, Katsuchi, Yamada, and Sasaki (2012) investigated the behaviour of airborne sea salt particles around bridge decks by wind tunnel tests using the particle image velocimetry (PIV) technique. Nakanishi, Kato, and Iwasaki (2011) also performed a study on local windborne sea salt adhesion distribution around a bridge girder section using wind tunnel experiments. Hasebe et al. (2012, 2015) predicted the behaviour of airborne sea salt on bridge girders using the image processing technique of flow visualization. Kato and Takeda (2000) investigated through numerical analysis the applicability of aerodynamic countermeasures on box girders. The Cooperative Research Centre (CRC) for Construction Innovation (2006) studied the effect of the height of bridge above water on salt deposition levels for bridges located near and farther from the coast.

There have been few studies related to reduction of airborne sea salt adhesion amount on bridge girders by aerodynamic countermeasures. The most commonly known countermeasures against corrosion by airborne sea salt are application of anti-corrosion paint which requires regular repainting depending on the severity of corrosion, and the use of weathering steel. The objective of this study is to reduce airborne sea salt adhesion amount on the surface of bridge girders by employing aerodynamic countermeasures to change the wind flow pattern around a bridge structure with an aim of reducing the wind velocity normal to the girders. The study bridge, employed because it is typical in metropolitan highways, is an I-shaped steel girder bridge with 8

京都大学 KYOTO UNIVERSITY
A Self-archived copy in
Kyoto University Research Information Repository
https://repository.kulib.kyoto-u.ac.jp
京都大学学術情報リポジトリ KURENAI 紅 Kyoto University Research Information Repository

girders. First, devices existing on urban highway bridges such as: noise barriers, median barriers, and facilities for passage of drainage pipes, electric cables, and railings used during bridge maintenance operations are investigated for their ability to reduce airborne sea salt adhesion amount. Noise barriers and median barriers, used to reduce the loudness of traffic noise and to mitigate median crossover accidents respectively, are easy to access and modify because they are located above the bridge deck. By changing the height of these barriers, reduction of airborne sea salt adhesion amount is investigated. Below the bridge deck, facilities for passage of drainage pipes, electric cables, and also railings used during bridge maintenance operations are visible. These are modelled as horizontal plates and by altering their position, their ability to reduce airborne sea salt adhesion amount is investigated. Subsequently, vertical plates are installed on the bridge girders as new devices to change the flow separation and the flow pattern around the bridge. Another aim of the present study is to ensure the installed aerodynamic countermeasure devices are short and as few as possible to be applicable in real practice. Additionally, achieving equal airborne sea salt adhesion amount on all girders is considered important to enhance effective maintenance because bridge maintenance is done simultaneously on all girders.

2. Methodology of airborne sea salt adhesion amount estimation

In the present study, numerical methods for flow field analysis and airborne sea salt adhesion amount estimation similar to the research by Noguchi et al. (2015), in which an I-shaped steel girder bridge having 3 main girders shown in Figure 1 was used to perform airborne sea salt adhesion amount analysis, are employed. The study bridge is located in Wakayama prefecture, Japan, on National Highway 42 and the bridge axis is NNW-SSE. At the WSW side is the Pacific Ocean and ENE side is a cliff.

京都大学 KYOTO UNIVERSITY
A Self-archived copy in
Kyoto University Research Information Repository
https://repository.kulib.kyoto-u.ac.jp
京都大学学術情報リポジトリ KURENAI 紅 Kyoto University Research Information Repository

At the bridge site, during the period 2011.3.7 - 2011.4.28, the recorded meteorological data is shown in Figure 2 and Figure 3. Airborne salinity concentration in the vicinity of the bridge was measured by tubular collecting devices installed perpendicular to the bridge axis oriented towards the WSW direction. For the above-mentioned period, the airborne salinity concentration, C, was determined as 0.01777 mg/m^3 (Noguchi et al., 2015).

2.1: Flow field analysis

To estimate the airborne sea salt adhesion amount on a bridge surface, it is important to analyse the flow field around the bridge structure. Noguchi et al. (2015) employed the standard k-ε turbulence model of Reynolds Averaged Navier Stokes (RANS) equations (Ferziger & Peric, 2002) to analyse the steady state flow field around an I-shaped steel girder bridge. 3D flow field around the study bridge model was investigated with consideration of the surrounding geography.

2.2: Airborne sea salt adhesion amount estimation

Airborne sea salt adhesion amount on the surface of the bridge girders was estimated by the improved concentration flux method which takes into account adhesion of airborne sea salt due to inertia and diffusion with consideration of gravity as expressed by the equation below (Kaneshiro et al., 2014). The first term corresponds to adhesion by inertia and the second term adhesion by diffusion.

$$Q = C \cdot \left(V_n + V_g \cos\theta\right) \cdot \Delta t \; + \; C \cdot \int_0^{\Delta t} \sqrt{\frac{D}{\pi t}}\, dt \qquad (1)$$

where Q: sea salt adhesion amount (mg/m^2), C: airborne salinity concentration (mg/m^3), V_n: wind velocity normal to a surface 35 mm away (m/s), V_g: terminal falling velocity of

京都大学 KYOTO UNIVERSITY
A Self-archived copy in
Kyoto University Research Information Repository
https://repository.kulib.kyoto-u.ac.jp
京都大学学術情報リポジトリ KURENAI 紅 Kyoto University Research Information Repository

a sea salt particles due to gravity (m/s), θ: wall inclination angle (rad), and D: diffusion coefficient (m^2/s).

Wind velocity normal to a surface, V_n, which should be close enough to the surface of each structural member, was determined by solving RANS equations using the previously stated standard k-ε turbulence model. For the diffusion coefficient, D, the coefficient of kinematic viscosity of air ($D = 1.5\times10^{-5}$ m^2/s) was adopted.

The washing-out effect due to rainfall which particularly affects the outer members of a bridge structure that are exposed to rainfall was evaluated by experimental analysis using I-sectional steel channel specimens and galvanised iron sheets. Noguchi et al. (2015) then determined the washing-out equation as:

$$S = 0.1231r^{-6.03} \times 100\ (\%) \qquad (2)$$

where S is the residual ratio of salinity (%) and r is the precipitation rate (mm/h). For the I-shaped steel girder bridge (Figure 1), the washing-out effect was applied on the sea side of the most upstream girder (positions ‘A’-‘D’) and on the cliff side of the most downstream girder (positions ‘a’-‘d’).

2.3: Comparison between observed and calculated sea salt adhesion amount

On the surface of the I-shaped steel girder bridge shown in Figure 1, measurements of local airborne sea salt adhesion amount were taken at positions ‘A’-‘d’. The measured values were then compared to values estimated by the improved concentration flux method and Figure 4 shows the results obtained. Based on the order and trend of sea salt adhesion amount between observed and estimated values, the improved concentration flux method is able to produce a satisfactory estimate of adhered airborne sea salt amount on the bridge girders. At some points however, there is a discrepancy between observed and calculated sea salt adhesion amount. This is speculated to arise from the fact that even though the flow field simulated by numerical analysis considers the

京都大学 KYOTO UNIVERSITY
A Self-archived copy in
Kyoto University Research Information Repository
https://repository.kulib.kyoto-u.ac.jp
京都大学学術情報リポジトリ KURENAI 紅 Kyoto University Research Information Repository

geography around the bridge, the flow field may not be exactly identical to the flow field on the real bridge because of accuracy of modelled topography such as the cliff and tetrapod structures along the coast. However, the present study will not take into account the surrounding topography. The reliability of the numerical methods employed as well as collected meteorological data and airborne salinity concentration can therefore be verified. Accordingly, the same numerical method for flow field analysis will be employed in the present study. Because of lack of data in the present study, the meteorological data and airborne salinity concentration will also be used.

3. Airborne sea salt adhesion on an I-shaped steel girder bridge

3.1: Study bridge

In the present study, an I-shaped steel girder bridge with 8 girders is employed for airborne sea salt adhesion amount analysis. The bridge is located in Osaka prefecture in Japan and is part of the Hanshin Expressway. As previously stated, this type of bridge section is selected because it is typical in many metropolitan highways.

The bridge is modelled using computer aided design (CAD) data and the cross section is shown in Figure 5. The height of the web is 2,390 mm with a thickness of 11 mm and the flange is 422.5 mm long and 20 mm thick. The spacing between girders is 2,939.7 mm and the bridge railings are 1,000 mm in height. The total width of the bridge, B, is 22,560 mm and the total height, D, is 3,735 mm. All the bridge girders are represented by G1-G8 respectively. Additionally, lateral members normally visible between the girders are excluded from the model to minimize complexity of the structure.

京都大学 KYOTO UNIVERSITY
A Self-archived copy in
Kyoto University Research Information Repository
https://repository.kulib.kyoto-u.ac.jp
京都大学学術情報リポジトリ KURENAI 紅 Kyoto University Research Information Repository

3.2: Two-dimensional flow field analysis

In contrast to the study by Noguchi et al. (2015) where 3D flow field analysis was performed, the present study takes into account 2D flow field analysis around the study bridge. This is in an effort to scale down the computational time load and also because comparison of sea salt adhesion amount estimated from 2D and 3D flow field analyses produced identical results.

3.2.1: Computational domain and boundary conditions

The size of the computational domain is decided by the total height of the bridge section, D. For the study bridge, the computational domain size is 134 m × 78 m ($36D \times 21D$) with a total of 263,456 grids. Details of the domain size are shown in Figure 6.

Respective initial and boundary conditions for steady state flow field analysis are shown in Table 1. At the inlet, an approaching wind velocity of 2 m/s perpendicular to the bridge axis is employed. This wind velocity was chosen because the study bridge has a rectangular cross-section with specific flow separation points and therefore the flow field isn't subject to any change even if the inlet wind velocity is varied.

3.2.2: Governing equations and calculation algorithm

The collocated grid system and the standard k-ε turbulence model are employed for steady state flow field analysis. This turbulence model is adopted also owing to its simplicity and good convergence rate (Versteeg & Malalasekera, 2007). For the wall function equation, the Spalding wall function is employed in which the velocity profile is essentially a fit of the viscous sublayer, buffer layer, and the log-law region (Spalding, 1961).

The advantage of this wall function is that grid points below the logarithmic region, $y^+<30$, can be solved without loss of precision limited with the validity of the

京都大学 KYOTO UNIVERSITY
A Self-archived copy in
Kyoto University Research Information Repository
https://repository.kulib.kyoto-u.ac.jp
京都大学学術情報リポジトリ KURENAI 紅 Kyoto University Research Information Repository

logarithmic velocity profile. The Semi-Implicit Method for Pressure Linked Equations (SIMPLE) method is used to perform iterative calculations until convergence.

3.3: Results of flow field analysis

Contour diagrams of time averaged wind velocity around the study bridge girders are shown in Figure 7. An anticlockwise wind circulation flow pattern is observed between the girders and comparison of contour diagram scales between the upstream and downstream sides of the bridge (G1-G4 and G5-G8) suggests that the flow gets stronger towards the downstream side.

Following flow field simulations, non-dimensional wind velocity normal to the bridge girders, described as V_n in the improved concentration flux equation (equation 1), is sampled around the bridge girders for use in airborne sea salt adhesion amount estimation. In the present study, the estimation points of airborne sea salt adhesion amount on the web and the flange of the girders are shown in Figure 8.

3.4: Airborne sea salt adhesion amount estimation

Airborne sea salt adhesion amount on the surface of the bridge girders is estimated according to the improved concentration flux method (equation 1). As previously stated, meteorological data and airborne salinity concentration from the study by Noguchi et al. (2015) are employed. The study bridge is therefore considered as being in the same location as the I-shaped steel girder bridge in the study by Noguchi et al. (2015) and the bridge axis remains NNW-SSE. Because the present study takes into account 2D flow field analysis around the study bridge, wind blowing from different directions is made perpendicular to the bridge axis by multiplying the wind velocity with the wall-normal component at different angles. The washing-out effect due to rainfall is not applied at this stage.

京都大学 KYOTO UNIVERSITY
A Self-archived copy in
Kyoto University Research Information Repository
https://repository.kulib.kyoto-u.ac.jp
京都大学学術情報リポジトリ KURENAI 紅 Kyoto University Research Information Repository

The distribution of airborne sea salt adhesion amount on selected girders on the upstream and downstream sides of the study bridge are shown in Figure 9. The results show that the sea salt adhesion amount on G1 is high and this can be attributed to direct collision of sea salt particles. On G2, the sea salt adhesion amount on the flange is higher than the web whereas on G5 and G6, there is more sea salt adhesion amount on the web compared to the flange. The pattern of sea salt adhesion amount distribution from G3 onwards is similar to the pattern observed on G5 and G6; however, the only difference is that on G3 the sea salt adhesion amount on the flange is comparatively higher than the web. Airborne sea salt adhesion amount per day integrated over the span of respective girders of the study bridge is shown in Figure 10. The integrated airborne sea salt adhesion amount at each sampling point (mg/m) is obtained by multiplying the sea salt adhesion amount estimated by the improved concentration flux method (mg/m^2) at that specific point with the distance (m) between the midpoints of adjacent sampling points. The total sea salt adhesion amount scale represents the cumulative sea salt adhesion amount on all girders. The study bridge is termed as original bridge because no aerodynamic countermeasures have been employed to reduce airborne sea salt adhesion amount. The most upstream girder, G1, has the highest amount of adhered airborne sea salt and it thus forms a significant percentage of the total airborne sea salt adhesion amount.

In the next chapter, aerodynamic countermeasures are employed to reduce the airborne sea salt adhesion amount on the study bridge. Reducing airborne sea salt adhesion amount implies that adhesion due to both inertia and diffusion be controlled. Because it is impossible to control the diffusion coefficient and also based on the assumption that adhesion by diffusion is rather low, reducing airborne sea salt adhesion amount requires reduction of adhesion by inertia. Therefore, by reducing the non-

京都大学 KYOTO UNIVERSITY
A Self-archived copy in
Kyoto University Research Information Repository
https://repository.kulib.kyoto-u.ac.jp
京都大学学術情報リポジトリ KURENAI 紅 Kyoto University Research Information Repository

dimensional wind velocity normal to the bridge girders, reduction of airborne sea salt adhesion amount can be speculated.

4. Investigation of aerodynamic countermeasures

4.1: Strategy and countermeasures

Aerodynamic countermeasures are employed to reduce the airborne sea salt adhesion amount on the study bridge. These countermeasures are employed to change the wind flow pattern around the bridge girders in an attempt to reduce the U_x and U_y components of wind velocity normal to the web and the flange respectively.

Several aerodynamic countermeasure devices are installed on the study bridge. The strategy to reduce the non-dimensional wind velocity around the bridge girders and consequently the airborne sea salt adhesion amount is to install aerodynamic countermeasures above and below the bridge deck. Above the bridge deck, noise barriers and median barriers are employed and below the bridge deck horizontal plates and vertical plates are used. Facilities for passage of drainage pipes, electric cables, and railings used during bridge maintenance are modelled as horizontal plates and vertical plates are employed as devices to change the flow separation.

The height of noise barriers and median barriers installed above the bridge deck is a multiple of the height of the study bridge railings. For horizontal and vertical plates installed below the bridge deck, the sizes are expressed in terms of the length of the flange of the study bridge because all of these plates are located on or close to the flange. The length of installed plates is denoted by LP and the length of flange of the study bridge by LF. After application of aerodynamic countermeasures, the results of estimated airborne sea salt adhesion amount are compared with the original bridge.

京都大学 KYOTO UNIVERSITY
A Self-archived copy in
Kyoto University Research Information Repository
https://repository.kulib.kyoto-u.ac.jp
京都大学学術情報リポジトリ KURENAI 紅 Kyoto University Research Information Repository

4.2: Noise barriers and median barriers

On metropolitan highways, noise barriers are installed to solve the problem of noise caused by high volumes of traffic. On the other hand, highway median barriers act as devices to mitigate crossover accidents from traffic moving in opposite directions. Noise barriers are commonly installed on both sides of the bridge deck and median barriers at the centre of the highway. Being above the bridge deck, both of these devices are easy to access as well as modify.

In the present study, noise barriers and median barriers are installed on the study bridge and by varying their height, reduction of airborne sea salt adhesion amount on the girders is investigated. With respect to the direction of oncoming wind, Figure 11 shows noise barriers installed at the leading edge (H_L) and trailing edge (H_T) and median barriers installed at the centre (H_C).

Figure 12 shows the results of noise barriers installed on both sides of the bridge deck with the median barrier height maintained at 1 m. According to the results, 5 m high noise barriers reduce the total airborne sea salt adhesion amount by approximately 9.5% and 3 m high noise barriers by approximately 6%. In both cases, there is however very little reduction of sea salt adhesion amount on G1 and G8. On G1, the sea salt adhesion amount is still high because of direct collision of sea salt particles. The contour diagram of time averaged wind velocity in the main flow direction for 5 m high noise barriers is shown in Figure 13. In comparison to the study bridge (Figure 7), the wind flow pattern between the girders remains relatively the same. Between G1 and G2 there is no big change in the contour diagrams however the wind circulation flow is comparatively less and this explains the little reduction of sea salt adhesion amount on G1. A similar situation is observed between G7 and G8. From G2 to G7, less wind circulation flow is observed between the girders and the contour diagrams also become

京都大学 KYOTO UNIVERSITY
A Self-archived copy in
Kyoto University Research Information Repository
https://repository.kulib.kyoto-u.ac.jp
京都大学学術情報リポジトリ KURENAI 紅 Kyoto University Research Information Repository

lighter in colour implying reduced non-dimensional wind velocity normal to the bridge girders, hence more reduction of airborne sea salt adhesion amount compared to G1 and G8.

Based on the results of 5 m high noise barriers, the next cases seek to investigate the effect of a single noise barrier installed only on one side of the bridge deck, a median barrier, and a combination of noise barriers with a median barrier. All the barriers installed are 5 m high and Figure 14 shows the results obtained. From the results, a single noise barrier installed only at the leading edge and a combination of noise barriers with a median barrier produce nearly the same results as noise barriers installed at the leading and trailing edges. For a single noise barrier installed on the trailing edge and also for a median barrier, more effect is observed on the upstream side from G2 to G4 however from G5 onwards the sea salt adhesion amount increases. Nonetheless, in all the cases the sea salt adhesion amount on the most upstream girder, G1, remains high and there is also very little change in the sea salt adhesion amount on the most downstream girder, G8.

In this section, results have shown that noise barriers and median barriers can also reduce airborne sea salt adhesion amount. For noise barriers installed above the bridge deck at the leading and trailing edges, reduction of sea salt adhesion amount can be attributed to less and weaker wind circulation flow observed between the girders. Because of this, the non-dimensional wind velocity normal to the girders is reduced. The same applies to a single noise barrier installed at the leading edge and for a combination of noise barriers with a median barrier.

4.3: Horizontal plates installed on bridge girders

Below bridge decks exists facilities for passage of drainage pipes, electric cables, and railings used during bridge maintenance. These facilities are normally located between

京都大学 KYOTO UNIVERSITY
A Self-archived copy in
Kyoto University Research Information Repository
https://repository.kulib.kyoto-u.ac.jp
京都大学学術情報リポジトリ KURENAI 紅 Kyoto University Research Information Repository

consecutive bridge girders or adjacent to the girders. In the present study, the above mentioned facilities are modelled as horizontal plates and installed on the study bridge. By altering the position of installed horizontal plates, reduction of airborne sea salt adhesion amount is investigated. All installed horizontal plates are of the same size as the flange of the study bridge i.e. LP = LF.

First, to determine the appropriate direction to install horizontal plates on the girders, two fundamental cases examined. The first case takes into account horizontal plates installed on all girders oriented towards the upstream direction illustrated by Case H1 in Figure 15 and the other case takes into account horizontal plates oriented towards the downstream direction illustrated by Case H2 in Figure 16. Results shown in Figure 17 suggest that from G1 to G3 horizontal plates oriented towards the upstream are more effective in reducing sea salt adhesion amount whereas from G4 onwards, horizontal plates oriented towards the downstream are more effective. In the former case, there is a significant reduction of sea salt adhesion amount on G1.

To confirm the results obtained above and to further analyse the appropriate direction to install horizontal plates, one more case is studied in which only a single horizontal plate at a time is installed on each girder. Two instances are then investigated with the horizontal plate oriented towards the upstream and downstream directions respectively. This is repeated for all 8 girders meaning a total of 16 cases and the obtained results are shown in Figure 18.

Results confirm that from G1 to G3, horizontal plates oriented towards the upstream lead to more sea salt adhesion amount reduction and from G5 onwards horizontal plates oriented towards the downstream are more effective. However, on G4 the sea salt adhesion amount is relatively the same in both instances meaning an almost equal reduction of sea salt adhesion amount. Figure 19 shows the sea salt adhesion

京都大学 KYOTO UNIVERSITY
A Self-archived copy in
Kyoto University Research Information Repository
https://repository.kulib.kyoto-u.ac.jp
京都大学学術情報リポジトリ KURENAI 紅 Kyoto University Research Information Repository

amount distribution for a single upstream-oriented horizontal plate on G1 and downstream-oriented horizontal plate on G5. In comparison to the original bridge (Figure 9), on G1 more reduction of sea salt adhesion amount is observed on the upstream side of the web, the upstream side of the upper flange, and the lower flange. On the downstream side of the upper flange and the downstream side of the web there is a slight reduction. A similar sea salt adhesion amount reduction pattern is observed on G2 and G3 for horizontal plates installed oriented towards the upstream. For a horizontal plate oriented towards the downstream on G5, sea salt adhesion amount reduction is observed on the downstream side of the upper flange. A similar reduction pattern follows from G6 onwards.

Having established the appropriate directions to install horizontal plates on the girders, a new case conforming to the directions is examined. This time, horizontal plates are installed oriented towards the upstream from G1 to G4, and downstream from G4 to G8 as illustrated by Case H3 in Figure 20. According to the results obtained shown in Figure 21, using the confirmed appropriate directions results in more sea salt adhesion amount reduction. The total sea salt adhesion amount reduction is approximately 27% and also the sea salt adhesion amount on all girders appears slightly uniform. However, the disadvantage is that many plates are necessary to achieve a considerable sea salt adhesion amount reduction.

Finally, horizontal plates installed between consecutive girders as illustrated by Case H4 in Figure 22 are investigated. From the results shown in Figure 23, the authors can tell that there is very little total sea salt adhesion amount reduction as the adhesion amount on all girders is almost the same as the original bridge. The only slight decrease of adhesion amount can be observed on G2 and from G6 onwards. The total reduction

京都大学 KYOTO UNIVERSITY
A Self-archived copy in
Kyoto University Research Information Repository
https://repository.kulib.kyoto-u.ac.jp
京都大学学術情報リポジトリ KURENAI 紅 Kyoto University Research Information Repository

of sea salt adhesion amount is approximately 4%. It is speculated that there is no change in the wind flow pattern between the girders in comparison to the study bridge.

In this section, results have established that horizontal plates can also reduce airborne sea salt adhesion amount on bridge girders depending on their position and orientation with respect to the oncoming wind direction. On the upstream side of the bridge structure, horizontal plates installed oriented towards the upstream are more effective whereas on the downstream side of the bridge structure, horizontal plates oriented towards the downstream are more effective. For horizontal plates installed between consecutive girders, reduction of sea salt adhesion amount is exceedingly small.

4.4: Vertical plates installed on bridge girders

In the previous section, results obtained established that several horizontal plates are necessary to achieve a considerable reduction of airborne sea salt adhesion amount. Furthermore, even though the adhesion amount on the most upstream girder, G1, was incredibly reduced, the reduction from G3 onwards was comparatively less. Therefore, to achieve more reduction of sea salt adhesion amount on both the upstream and downstream sides of the bridge, vertical plates are installed. The aim of installing vertical plates is to change the flow separation below the bridge deck which will influence change of the wind flow pattern between the girders and the non-dimensional wind velocity normal to the girders. Vertical plates are mainly installed on the most upstream girder and several fundamental cases are considered during installation namely: first phase flow separation, vertical plate with a slit, second phase flow separation, and vertical plates between girders.

京都大学 KYOTO UNIVERSITY
A Self-archived copy in
Kyoto University Research Information Repository
https://repository.kulib.kyoto-u.ac.jp
京都大学学術情報リポジトリ KURENAI 紅 Kyoto University Research Information Repository

4.4.1: First phase flow separation

In this case, a single vertical plate of length LP is installed on the most upstream girder, G1, as illustrated by Case V1 in Figure 24. As the installed vertical plate is elongated, it will lower the flow separation point below the bridge deck and the separation of flow at this stage is termed as first phase flow separation.

According to the obtained results shown in Figure 25, there is more reduction of total airborne sea salt adhesion amount as the vertical plate is elongated. However, on the upstream side of the bridge from G1 to G3, there is no big difference in sea salt adhesion amount as the vertical plate is elongated because G1, G2, and G3 are in the wake region. On the other hand, on the downstream side from G5 onwards more sea salt adhesion amount reduction is observed as the vertical plate is elongated because for long vertical plates reattachment of the flow separated on the most upstream girder occurs further downstream compared to short vertical plates. Installing an extremely long vertical plate on the most upstream girder is however not applicable in real practice. For a vertical plate twice the length of the flange, LP = 2LF, the total sea salt adhesion amount reduction is approximately 47%. For this case, the contour diagram of time averaged wind velocity in the main flow direction on the upstream side of the bridge is shown in Figure 26.

From the contour diagram, it is evident that with a vertical plate on the most upstream girder, the point of flow separation is lowered and as a result the wind flow pattern between the girders, especially on the upstream side of the bridge, changes. A large anti-clockwise circulation flow is formed right below girders G1, G2, and G3 and a weak clockwise circulation flow is observed between G1 and G2. From G2 onwards to G4, the wind circulation flow pattern between the girders is greatly diminished and weaker in comparison to the study bridge (Figure 7). The downstream side from G5

京都大学 KYOTO UNIVERSITY
A Self-archived copy in
Kyoto University Research Information Repository
https://repository.kulib.kyoto-u.ac.jp
京都大学学術情報リポジトリ KURENAI 紅 Kyoto University Research Information Repository

onwards is characterised by wind flow pattern that is similar but weaker than the study bridge. All these explain the reduction of sea salt adhesion amount because of reduced non-dimensional wind velocity normal to the bridge girders. Because of the diminished and weakened wind circulation flow between the girders especially on the upstream side of the bridge, the sea salt adhesion amount on the web is greatly reduced.

4.4.2: Vertical plate with a slit

To conform to the objective of employing short aerodynamic countermeasure devices, the vertical plate installed on the most upstream girder is shortened. This is done by introducing a slit between the flange and the installed vertical plate. In the previous sub-section, a vertical plate of length LP = 2LF installed on the most upstream girder was found to reduce the total airborne sea salt adhesion amount by approximately 47%. This vertical plate is shortened by introducing a slit of length LS illustrated by Case V2 in Figure 27.

The results of estimated airborne sea salt adhesion amount are shown in Figure 28. As per the results, it is clear that as the slit becomes wider the sea salt adhesion amount on the girders increases. On the most upstream girder the increase is particularly high because the opening created by the slit allows for more sea salt adhesion on the flange. Nonetheless, for a vertical plate with a slit of length LS = LF there is not much difference when compared with a solid vertical plate, LS = 0. Despite the increased sea salt adhesion amount on G1, the adhesion amount on G2 is even lower and on G3 the adhesion amount is relatively the same. On the downstream side from G4 onwards, the sea salt adhesion amount is slightly higher than the case with a solid vertical plate. The total sea salt adhesion amount reduction is approximately 41% which is 6% less that the case with a solid vertical plate. For the vertical plate with a slit of length LS = LF, the

京都大学 KYOTO UNIVERSITY
A Self-archived copy in
Kyoto University Research Information Repository
https://repository.kulib.kyoto-u.ac.jp
京都大学学術情報リポジトリ KURENAI 紅 Kyoto University Research Information Repository

contour diagram of time averaged wind velocity in the main flow direction on the upstream side of the bridge is shown in Figure 29.

The contour diagram indicates that with the introduction of a slit, the wind circulation flow between the girders from G1 to G4 is equally greatly diminished and weakened in comparison to the study bridge (Figure 7). The only visible but weak circulation flow is observed below the girders between G1 and G2 and G2 and G3. In comparison to the case with a solid vertical plate on G1 (Figure 26), the wind circulation flow between G1 and G2 is diminished and weakened more hence even lower sea salt adhesion amount on G2.

4.4.3: Second phase flow separation

In the previous two subsections, a single vertical plate was installed on the most upstream girder and the separation of flow was termed as first phase flow separation. On the downstream side of the bridge structure from G5 onwards, it was however noted that the airborne sea salt adhesion amount started to increase because of reattachment of the separated flow. For instance, for the case with a vertical plate of length LP = 2LF installed on G1, the sea salt adhesion amount progressively increases from G5 onwards as seen in Figure 25. Therefore, in this sub-section the possibility of re-separating the reattaching flow, termed as second phase flow separation, is investigated by installing an additional vertical plate on the downstream side of the bridge. For the case with a vertical plate of length LP = 2LF on G1, an additional vertical plate is installed on G5 which is the flow reattachment point. Installation of the additional vertical plate is illustrated by Case V3 in Figure 30.

In accordance with the results obtained shown in Figure 31, for additional vertical plates of up to length LP’ = 2LF the reduction of sea salt adhesion amount on the bridge girders is non-significant. The total values of sea salt adhesion amount also

京都大学 KYOTO UNIVERSITY
A Self-archived copy in
Kyoto University Research Information Repository
https://repository.kulib.kyoto-u.ac.jp
京都大学学術情報リポジトリ KURENAI 紅 Kyoto University Research Information Repository

remain more or less the same. The effect of the additional vertical plate starts to be noticed when the vertical plate is of length LP' = 3LF with a considerable reduction of sea salt adhesion amount observed when the vertical plate is of length LP' = 4LF. Therefore, it is concluded that for second phase flow separation to be successful an additional vertical plate longer that the vertical plate installed on the most upstream girder is inevitable on the downstream side of the bridge structure.

4.4.4: Vertical plates between girders

Until now, vertical plates have been installed on the flange of the bridge girders. In this sub-section, the effect of vertical plates installed between consecutive girders on the wind flow pattern between the girders as well as airborne sea salt adhesion amount is investigated. The installation of vertical plates is illustrated by Case V4 in Figure 32 and results obtained are shown in Figure 33.

It is evident that there is more sea salt adhesion amount reduction as the vertical plates are elongated and also there is a significant reduction on the downstream side of the bridge. On the most upstream girder, the reduction of sea salt adhesion amount is rather less because of direct collision of sea salt particles. On the downstream side of the bridge, long vertical plates however result in an increase of sea salt adhesion amount. The sea salt adhesion amount distribution on G6 and G7 for vertical plates of length LP = 0.5LF and LP = LF are compared in Figure 34 to establish the reason for increased adhesion amount on the downstream side of the bridge.

From the sea salt adhesion amount distribution plots, the main difference noted between vertical plates of length LP = 0.5LF and LP = LF is the adhesion amount on the upstream side of the upper flange where the case with vertical plates of length LP = LF has higher adhesion amount. This is the main reason for increase of sea salt adhesion amount on the downstream side of the bridge as installed vertical plates are made longer.

京都大学 KYOTO UNIVERSITY
A Self-archived copy in
Kyoto University Research Information Repository
https://repository.kulib.kyoto-u.ac.jp
京都大学学術情報リポジトリ KURENAI 紅 Kyoto University Research Information Repository

It is therefore recommended that relatively shorter vertical plates be installed between the girders on the downstream side of the bridge. However, in both cases in Figure 34 the sea salt adhesion amount on the web is greatly reduced. The contour diagram of time averaged wind velocity in the main flow direction for the case with vertical plates of length LP = LF installed between the girders is shown in Figure 35.

According to the contour diagrams, the installed vertical plates have an effect of disrupting the flow entering the cavity between the girders. This weakens the wind circulation flow pattern between the girders, hence reduced non-dimensional wind velocity normal to the girders. The significant reduction of sea salt adhesion amount on the web can be explained by this.

5. Combination of aerodynamic countermeasure devices

Several aerodynamic countermeasures have so far been implemented to reduce the airborne sea salt adhesion amount on the study bridge. Results have established that vertical plates installed on the most upstream girder substantially reduce the sea salt adhesion amount on the bridge girders because of lowered flow separation that changes the wind flow pattern between the girders especially on the upstream side of the bridge. On the downstream side of the bridge, because of reattachment of the separated flow the sea salt adhesion amount is however comparatively higher than on the upstream side of the bridge.

In this chapter, through combination of aerodynamic countermeasure devices reducing the total airborne sea salt adhesion amount by half is set as the target. Since the total sea salt adhesion amount of the study bridge is approximately 555.8 mg/m/day, 50% reduction means a total sea salt adhesion amount of approximately 277.9 mg/m/day which translates to an approximated uniform sea salt adhesion amount of 34.74 mg/m/day on each girder. This value represents our target value and the airborne

京都大学 KYOTO UNIVERSITY
A Self-archived copy in
Kyoto University Research Information Repository
https://repository.kulib.kyoto-u.ac.jp
京都大学学術情報リポジトリ KURENAI 紅 Kyoto University Research Information Repository

sea salt adhesion amount on each girder except G1 and G8, can only be equal to or less than the target value. G1 and G8 are treated as exceptions because with application of the washing-out effect due to rain, the sea salt adhesion amount is bound to decrease considerably.

For a vertical plate with a slit of length LS = LF on the most upstream girder (Figure 27), two additional vertical plates are installed between girders G5, G6, and G7 where the sea salt adhesion amount is above the target value. Installation of the additional vertical plates is illustrated by Case V5 in Figure 36 and the results obtained are shown in Figure 37. According to the results, a pair of additional vertical plates of length LP = 0.5LF installed between girders G5, G6 and G7 sufficiently lower the adhesion amount to values less than the desired target value. The total reduction of adhesion amount is approximately 47% which is an improvement from the previous result of 41% with no additional vertical plates on the downstream side. The contour diagram of time averaged wind velocity in the main flow direction is shown in Figure 38. In comparison to the original bridge (Figure 7), there is less and weaker wind circulation flow observed between the girders. The light-coloured nature of the contour diagram also confirms change of the flow field and that the non-dimensional wind velocity normal to the bridge girders is significantly lower than the study bridge.

To reduce the airborne sea salt adhesion amount on G1 and G8, the washing-out effect due to rain is applied on the outer surfaces of G1 and G8 according to equation (2) and the results obtained are shown in Figure 39. As expected, the sea salt adhesion on G1 and G8 is significantly reduced and the total reduction of sea salt adhesion amount is approximately 60%. Furthermore, the obtained sea salt adhesion amount on each girder is relatively uniform.

京都大学 KYOTO UNIVERSITY
A Self-archived copy in
Kyoto University Research Information Repository
https://repository.kulib.kyoto-u.ac.jp
京都大学学術情報リポジトリ KURENAI 紅 Kyoto University Research Information Repository

6. Conclusions

In the present study, aerodynamic countermeasure devices have been employed to reduce the airborne sea salt adhesion amount on an I-shaped steel girder bridge typical in metropolitan highways. Devices existing on urban highway bridges such as noise barriers, median barriers, and facilities for passage of drainage pipes, electric cables, and railings used during bridge maintenance, modelled as horizontal plates, have been investigated for their ability to also reduce airborne sea salt adhesion amount. As additional devices, vertical plates installed on the bridge girders have also been studied. CFD has been employed for flow field simulations and airborne sea salt adhesion amount has been estimated by the improved concentration flux method. The following conclusions are drawn:

(1) Noise barriers and median barriers installed above the bridge deck can also reduce airborne sea salt adhesion amount on bridge girders. Noise barriers installed at the leading and trailing edges weaken the wind circulation flow pattern between the girders thereby reducing the non-dimensional wind velocity normal to the girders that leads to reduced sea salt adhesion amount. In the present study, 5m high noise barriers could reduce the total sea salt adhesion amount by approximately 9.5%.

(2) On highway bridges, facilities for passage of drainage pipes, electric cables, and railings used during bridge maintenance can also reduce airborne sea salt adhesion amount by varying their position with respect to the direction of oncoming wind. These facilities, modelled as horizontal plates, are more effective when installed oriented towards the upstream on the upstream side of the bridge, and downstream on the downstream side of the bridge. For horizontal

京都大学 KYOTO UNIVERSITY
A Self-archived copy in
Kyoto University Research Information Repository
https://repository.kulib.kyoto-u.ac.jp
京都大学学術情報リポジトリ KURENAI 紅 Kyoto University Research Information Repository

plates installed between bridge girders, the reduction of sea salt adhesion amount is minimal.

(3) A vertical plate installed on the flange of the most upstream girder lowers the flow separation point and changes the wind flow pattern on the upstream side of the bridge. The wind circulation flow pattern on the upstream side of the bridge is diminished and weakened hence reduced non-dimensional wind velocity normal to the bridge girders and less airborne sea salt adhesion amount. Because of reattachment of the separated flow on the downstream side of the bridge, the sea salt adhesion amount is however higher than the upstream side. In the present study, a vertical plate twice the length of the flange was found to reduce the total sea salt adhesion amount by approximately 47%. Introduction of a slit to the vertical plate installed on the most upstream girder also weakens the wind circulation flow pattern on the upstream side of the bridge. Employing an additional vertical plate for second phase flow separation on the downstream side of the bridge to reduce the sea salt adhesion amount caused by flow reattachment requires a vertical plate longer than the one installed on the most upstream girder.

(4) Vertical plates installed between bridge girders disrupt the entry of flow into the cavity between the girders and weaken the circulation flow pattern between the girders thereby reducing the non-dimensional wind velocity normal to the girders. As a result, the airborne sea salt adhesion amount on the web is significantly reduced. However, on the downstream side of the bridge long vertical plates installed between the girders have an effect of increasing the sea salt adhesion amount. Therefore, on the downstream side of the bridge installation of relatively shorter vertical plates between girders is recommended.

京都大学 KYOTO UNIVERSITY
A Self-archived copy in
Kyoto University Research Information Repository
https://repository.kulib.kyoto-u.ac.jp
京都大学学術情報リポジトリ KURENAI 紅 Kyoto University Research Information Repository

(5) A combination of a vertical plate with a slit installed on the most upstream girder with short vertical plates installed between girders on the downstream side of the bridge further reduces the airborne sea salt adhesion amount on the downstream side of the bridge as well as the total sea salt adhesion amount.

(6) More than 50% reduction of total airborne sea salt adhesion amount can be realised by applying the washing-out effect on the outer surfaces of the most upstream and downstream girders to the results obtained in (5). In the present study, by applying the washing-out effect uniform sea salt adhesion amount on all the girders was also achieved.

In future, it is important to consider 3D flow field analysis around the bridge structure inclusive of lateral members.

Acknowledgements

This work was partially supported by JSPS KAKENHI under Grant 15H02261 and 16J09269. The authors would also like to express their gratitude to Mr. Soichiro HATA for his contribution towards making this work a success.

京都大学 KYOTO UNIVERSITY
A Self-archived copy in
Kyoto University Research Information Repository
https://repository.kulib.kyoto-u.ac.jp
京都大学学術情報リポジトリ KURENAI 紅 Kyoto University Research Information Repository

References

Chen, Y., Chiu, H., Chan, Y., Chang, Y., & Yang, C. (2012). Prediction of air-borne salt distribution in the coastal region of northern Taiwan. *Journal of Marine Science and Technology*, Vol. 20, No. 3, 259-268.

Cole, L.S., Lau, D., Chan, F., & Paterson, D.A. (2013). Experimental studies of salts removal from metal surfaces by wind and rain. *Corrosion Engineering, Science and Technology*, Vol. 39, No. 4, 333-338.

Cooperative Research Centre for Construction Innovation (2006). *Effect of Height of Bridge Above Water on Salt Deposition Levels*. Brisbane, Australia.

Corvo, F., Betancourt, N., & Mendoza, A. (1995). The influence of airborne salinity on the atmospheric corrosion of steel. *Corrosion Science*, Vol. 27, No. 12, 1889-1901.

Ferziger, J.H., & Peric, M. (2002). *Computational Methods for Fluid Dynamics*. Newyork: Springer.

Hasebe, H., Kosugi, T., Hatamoto, S., Kawai, T., Nakayama, S., & Nomura, T. (2012). Image Processing Technique of Flow Visualization For the Prediction of Airborne Salt Behavior Around A Bridge Girder. *22nd Wind Engineering Symposium*, 353-358 (in Japanese).

Hasebe, H., Sakakibara, Y., Yamaya, K., Sone, R., Haruki, Y., & Nomura, T. (2015). Wind tunnel experiment to estimate the amount of airborne sea salt adhering to the surface of a bridge. (2015, June). *14th International Conference on Wind Engineering, Porto-Alegre, Brazil*.

Kaneshiro, Y., Noguchi, K., Hata, S. & Kang, Y. (2014). Estimation of air-borne sea salt deposition by numerical simulation. *23rd Wind Engineering Symposium,* 511-516 (in Japanese).

Lovett, R.F. (1978). Quantitative measurement of airborne sea-salt in the North Atlantic. *Tellus*, 30, 358-364.

Kato, M., & Takeda, K. (2000). Application of numerical analysis of windborne salt to the bridge design. Trial to expand the applicability of weathering steel. *Steel Construction Engineering*, Vol. 7, No. 8, 45-54 (in Japanese).

Manders, A.M.M., Schaap, M., Querol, X., Albert, M.F.M.A., Vercauteren, J., Kuhlbusch, R., & Hoogerbrugge, R. (2010). Sea salt concentrations across the European continent. *Atmospheric Environment*, 44, 2434-2442.

Nakanishi, K., Kato, M., & Iwasaki, E. (2011). Fundamental study on local windborne adhesion distribution around a bridge girder section using wind tunnel experiment. *Journal of Japanese Society of Civil Engineers A1* (*Structures, Earthquake engineering*), Vol. 67, No. 2, 326-335 (in Japanese).

Noguchi, K., Kang Y., Okuda S., Kurata N., Shirato H., & Yagi, T. (2013). Study on improvement of estimation accuracy of amount of air-borne sea salt adhered to a structural surface. *Journal of Structural Engineering*, Vol. 59A, 585-595 (in Japanese).

京都大学 KYOTO UNIVERSITY
A Self-archived copy in
Kyoto University Research Information Repository
https://repository.kulib.kyoto-u.ac.jp
京都大学学術情報リポジトリ KURENAI 紅 Kyoto University Research Information Repository

Noguchi K., Kaneshiro, Y., Kang, Y., Shirato, H., Yagi, T., & Hattori, H. (2014). Evaluation of amount of salinity on structural surface based on physical behavior of sea salt particles and wind state. *Journal of Structural Engineering*, Vol. 60A, 613-621 (in Japanese).

Noguchi, K., Shirato, H., Yagi, T., Kaneshiro, Y., Hata, S., & Hattori, H. (2015, June). Quantitative evaluation of salinity on structural members in coastal region. *14th International Conference on Wind Engineering, Porto-Alegre, Brazil*.

Obata, M., Li, G., Watanabe, Y., & Goto, Y. (2014). Numerical simulation of adhesion of sea-salt particles on bridge girders. *Structure and Infrastructure Engineering,* Vol. 10, No. 3, 398-408.

Ronald, C., Katsuchi, H., Yamada, H., & Sasaki, H. (2012). Study on estimation of amount of airborne sea salt around bridge deck. *Journal of Structural Engineering*, Vol.58A, 528-541 (in Japanese).

Spalding, D.B. (1961). A single formula for the law of the wall. *Journal of Applied Mechanics*, 28, 455-458.

The Ministry of Land, Infrastructure, Transport and Tourism. (2013). http://www.mlit.go.jp/road/sisaku/yobohozen/yobo1_1.pdf (in Japanese).

Transportation for America (2010). *The Fix We're in For: The State of Our Nation's Bridges*. Washington, D.C

Versteeg, H.K., & Malalasekera, W. (2007). *An Introduction to Computational Fluid Dynamics. The Finite Volume Method.* Harlow: Pearson Education Limited.

京都大学 KYOTO UNIVERSITY
A Self-archived copy in
Kyoto University Research Information Repository
https://repository.kulib.kyoto-u.ac.jp
京都大学学術情報リポジトリ KURENAI 紅 Kyoto University Research Information Repository

Table 1. Initial and boundary conditions for two-dimensional steady state flow field analysis around the study bridge

	Inlet	Outlet	Upper boundary	Lower boundary
U	U = (2,0)	$\frac{\partial U}{\partial n} = 0$	Slip	Slip
p	$\frac{\partial p}{\partial n} = 0$	p = 0	$\frac{\partial p}{\partial n} = 0$	$\frac{\partial p}{\partial n} = 0$
k	0.015	$\frac{\partial k}{\partial n} = 0$	$\frac{\partial k}{\partial n} = 0$	$\frac{\partial k}{\partial n} = 0$
ε	1.935×10^{-5}	$\frac{\partial \varepsilon}{\partial n} = 0$	$\frac{\partial \varepsilon}{\partial n} = 0$	$\frac{\partial \varepsilon}{\partial n} = 0$

A Self-archived copy in
Kyoto University Research Information Repository
https://repository.kulib.kyoto-u.ac.jp

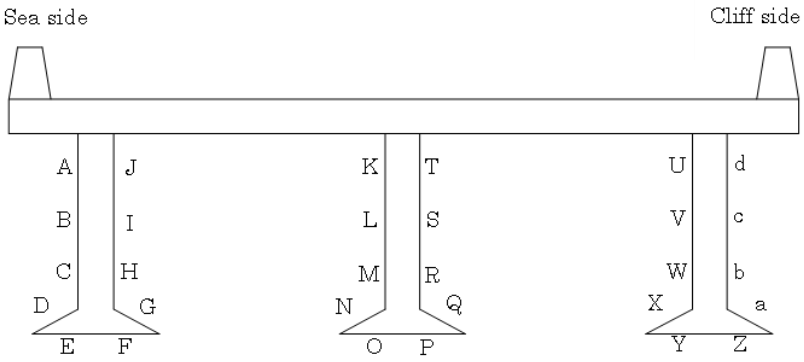

Figure 1. Cross-section of the I-shaped steel girder bridge showing measurement positions of airborne sea salt adhesion amount

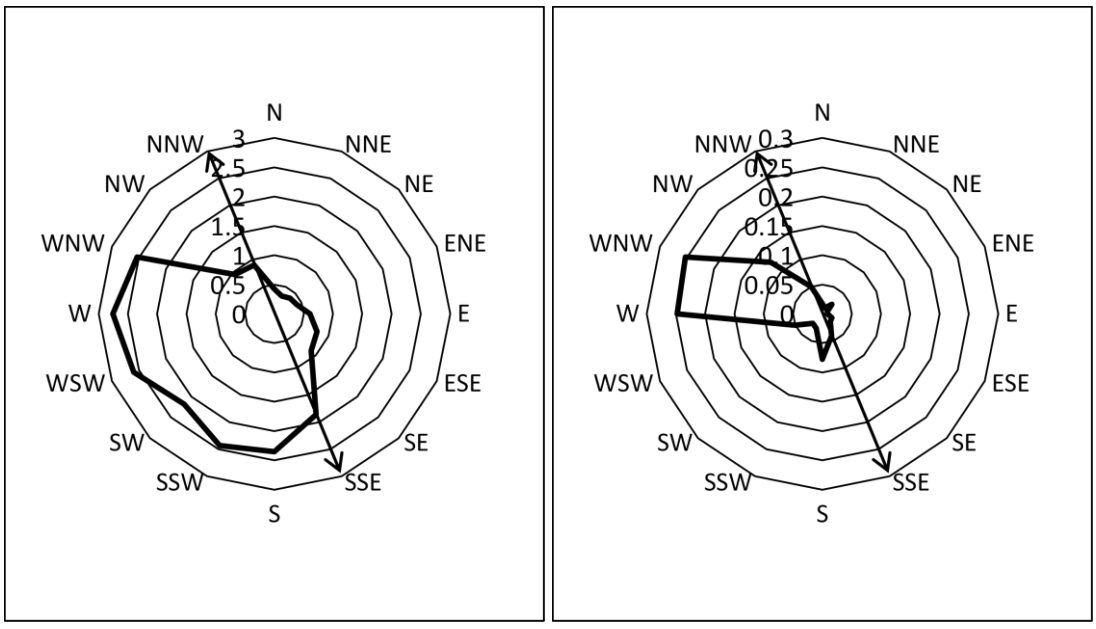

(a) (b)

Figure 2. Data observed by meteorological equipment in the study by Noguchi et al. (2015) during the period 2011.3.7 – 2011.4.28. (a) 10 minutes average wind speed and (b) 10 minutes prevailing wind direction. The bridge axis is shown by the arrow from NNW-SSE.

京都大学 KYOTO UNIVERSITY
A Self-archived copy in
Kyoto University Research Information Repository
https://repository.kulib.kyoto-u.ac.jp
京都大学学術情報リポジトリ KURENAI 紅 Kyoto University Research Information Repository

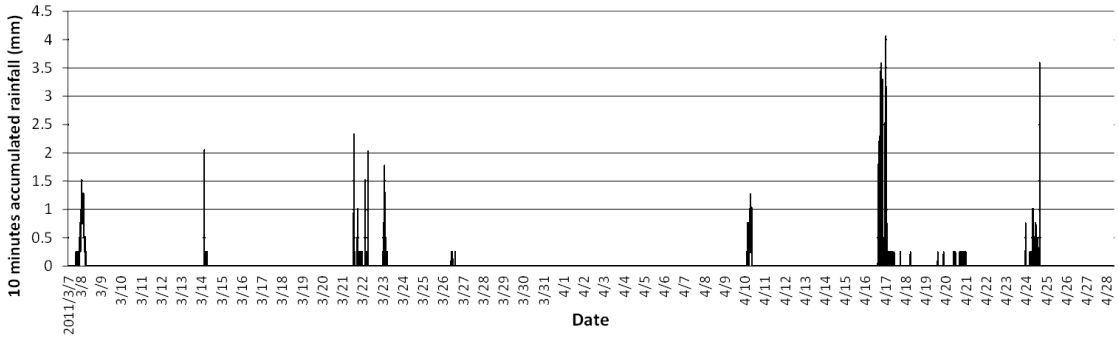

Figure 2. 10 minutes accumulated rainfall during the period 2011.3.7 – 2011.4.28

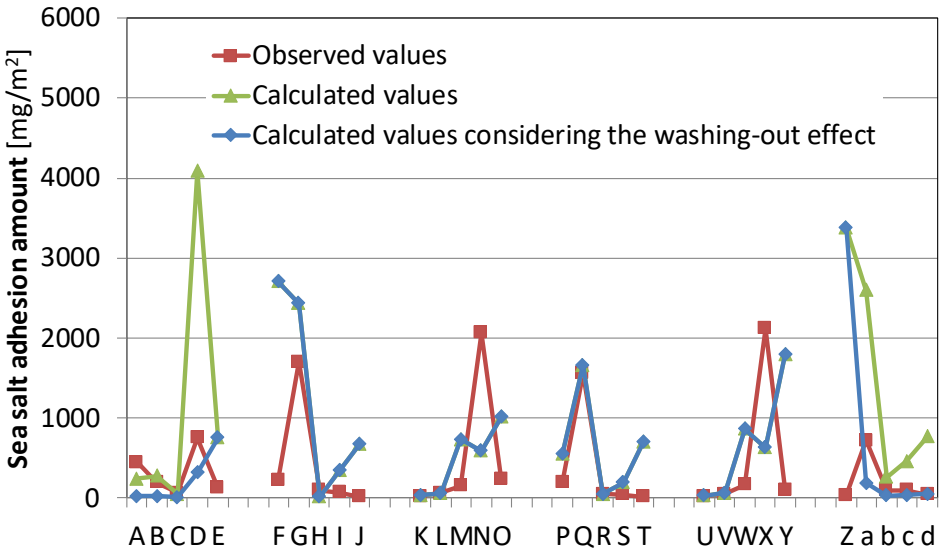

Figure 4. Comparison between observed and calculated values of airborne sea salt adhesion amount on the surface of the I-shaped steel girder bridge shown in Figure 1

京都大学 KYOTO UNIVERSITY
A Self-archived copy in
Kyoto University Research Information Repository
https://repository.kulib.kyoto-u.ac.jp
京都大学学術情報リポジトリ KURENAI 紅 Kyoto University Research Information Repository

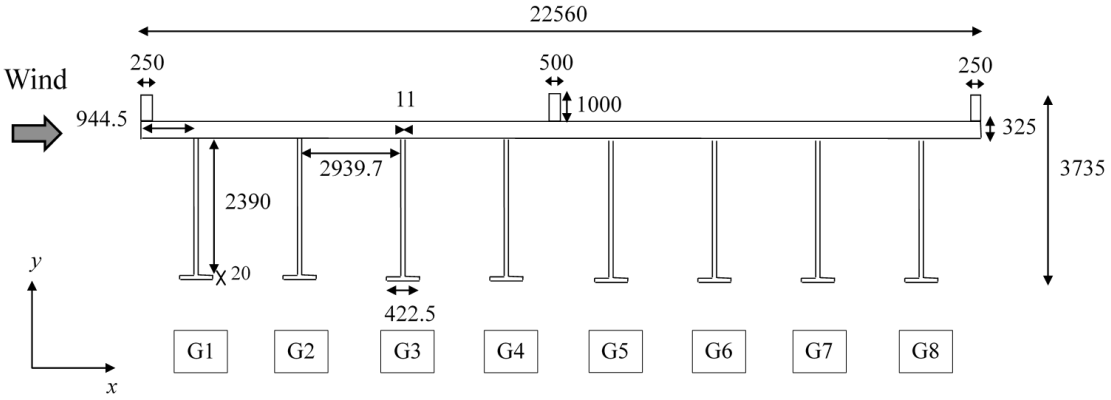

Figure 5. Cross-section of the study bridge in present research

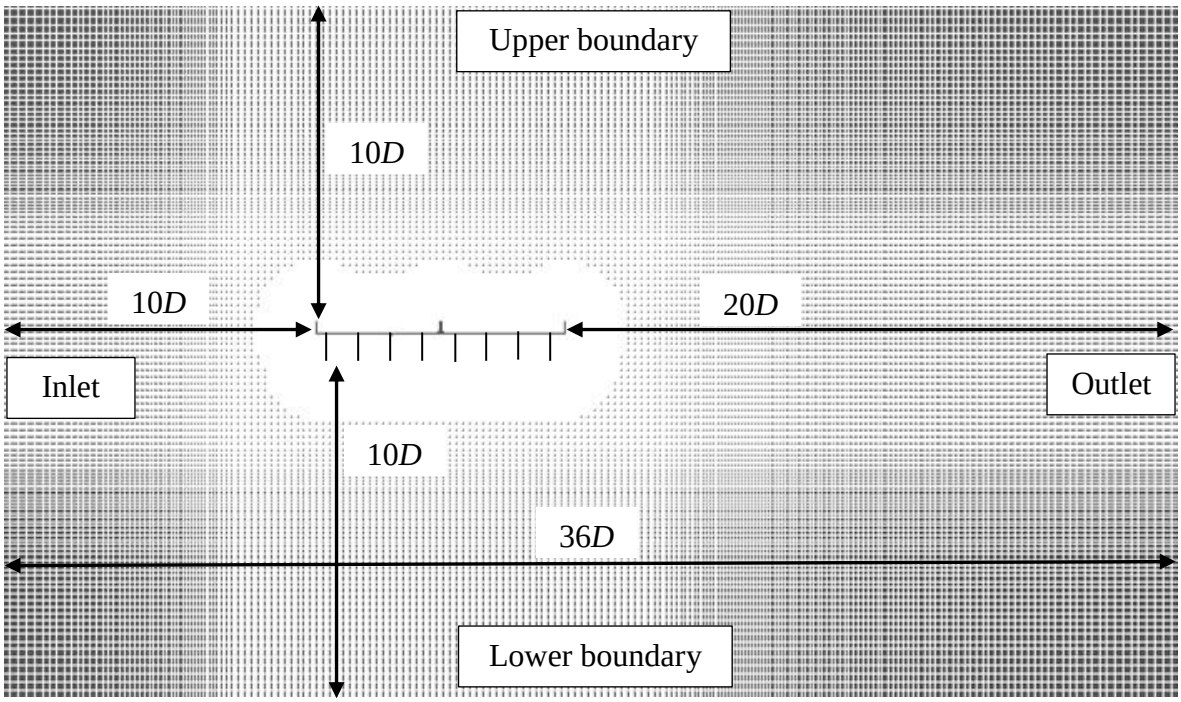

Figure 6. 2D computational domain for flow field analysis around the study bridge shown in Figure 5

京都大学 KYOTO UNIVERSITY
A Self-archived copy in
Kyoto University Research Information Repository
https://repository.kulib.kyoto-u.ac.jp
京都大学学術情報リポジトリ KURENAI 紅 Kyoto University Research Information Repository

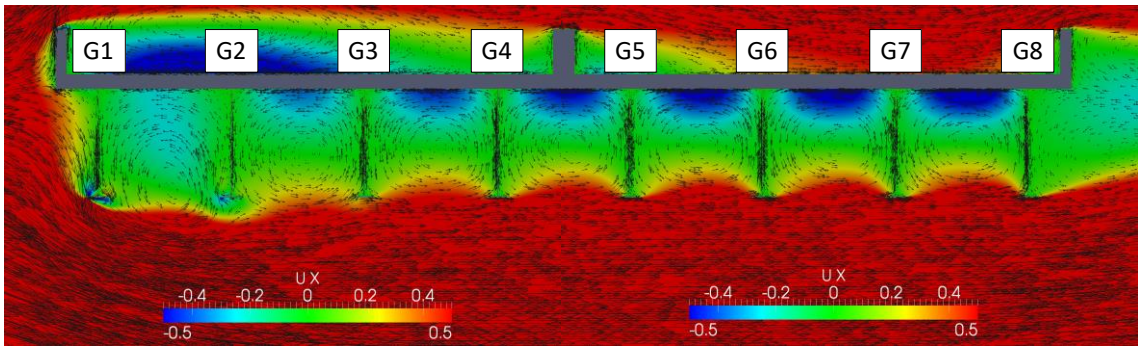

(a) Main flow direction

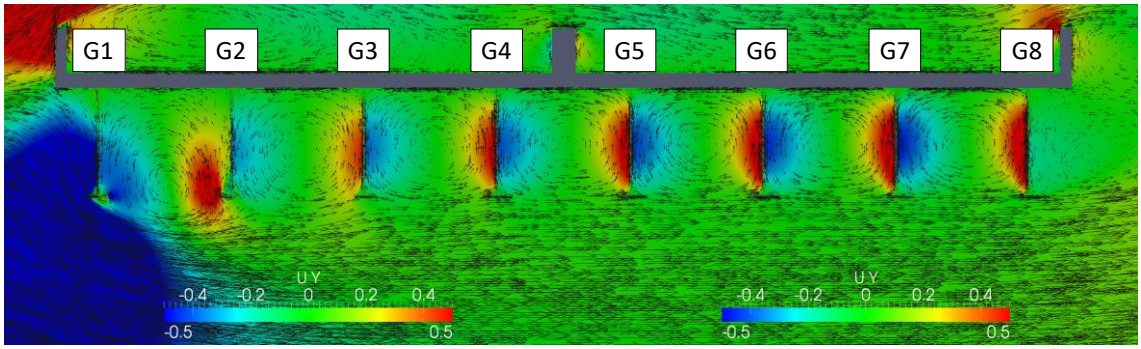

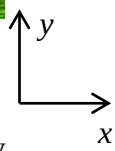

(b) Vertical direction

Figure 7. Contour diagrams of time averaged wind velocity (m/s) around the study bridge shown in Figure 5

京都大学 KYOTO UNIVERSITY
A Self-archived copy in
Kyoto University Research Information Repository
https://repository.kulib.kyoto-u.ac.jp
京都大学学術情報リポジトリ KURENAI 紅 Kyoto University Research Information Repository

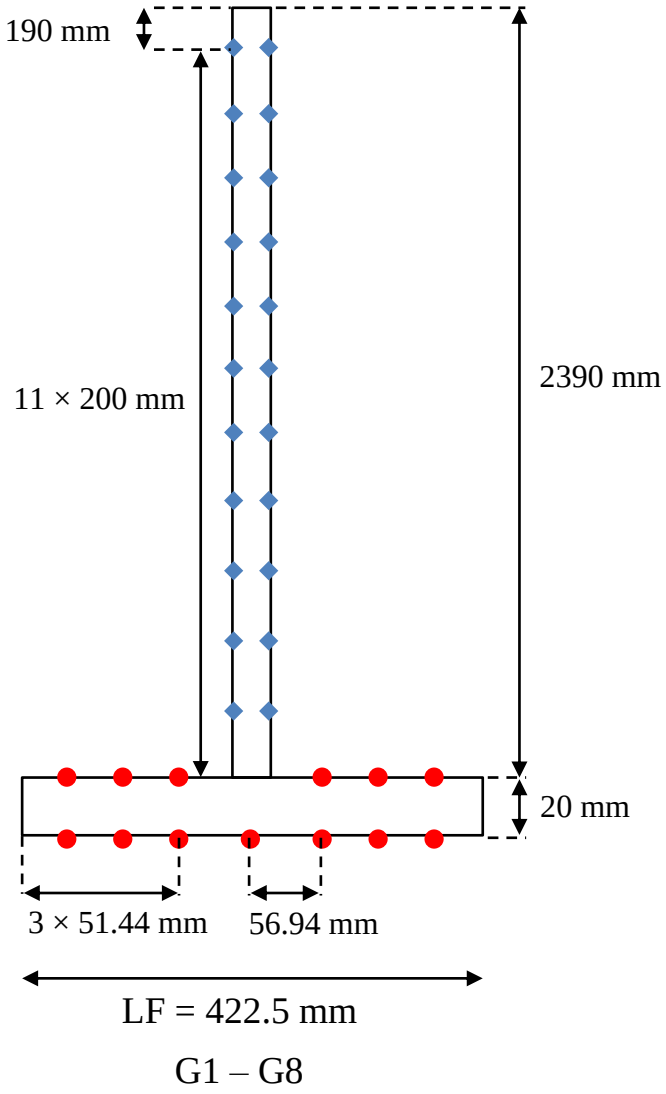

Figure 8. Estimation points of airborne sea salt adhesion amount on the surface of the bridge girders

京都大学 KYOTO UNIVERSITY
A Self-archived copy in
Kyoto University Research Information Repository
https://repository.kulib.kyoto-u.ac.jp
京都大学学術情報リポジトリ KURENAI 紅 Kyoto University Research Information Repository

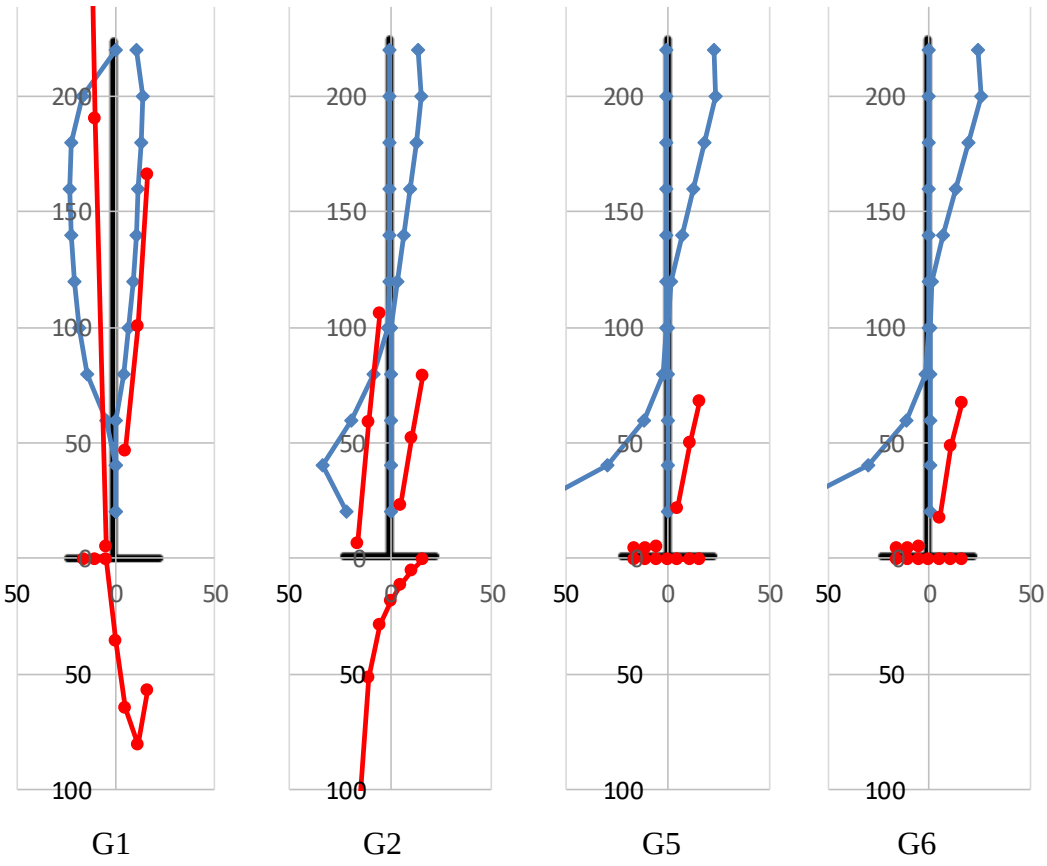

Figure 9. Distribution of sea salt adhesion amount (mg/m^2/day) around selected girders of the study bridge shown in Figure 5

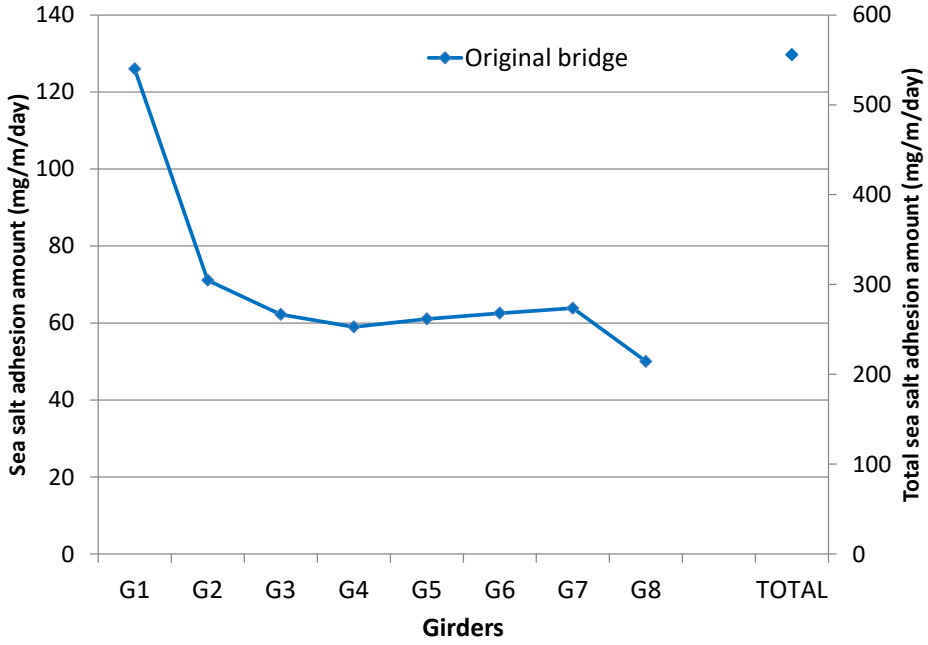

Figure 10. Airborne sea salt adhesion amount integrated over the span of corresponding girders of the study bridge shown in Figure 5

京都大学 KYOTO UNIVERSITY
A Self-archived copy in
Kyoto University Research Information Repository
https://repository.kulib.kyoto-u.ac.jp
京都大学学術情報リポジトリ KURENAI 紅 Kyoto University Research Information Repository

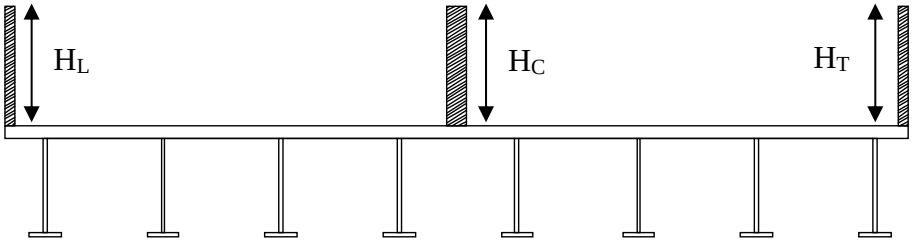

Figure 11. Illustration of noise barriers and a median barrier installed above the bridge deck

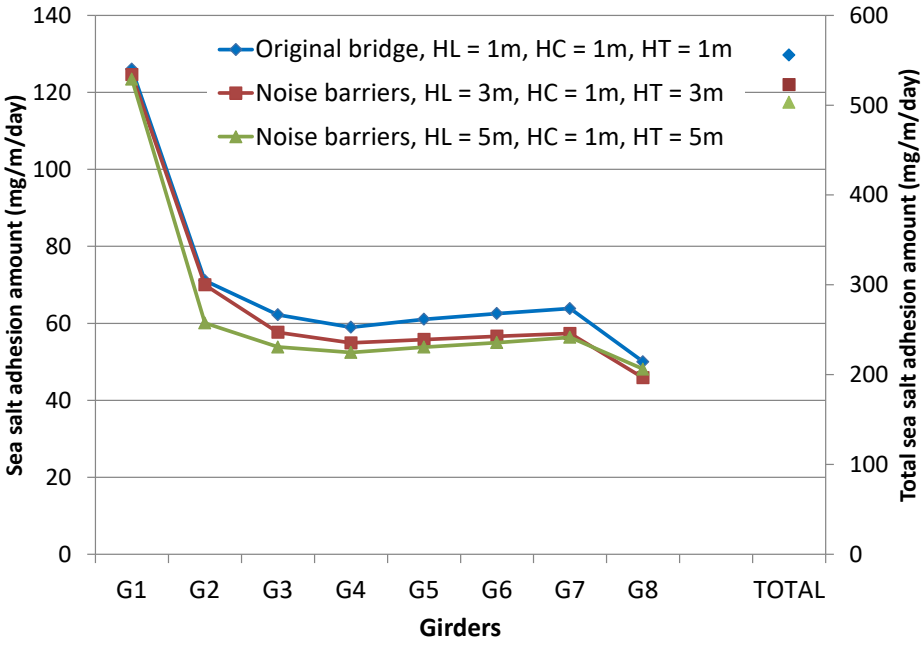

Figure 12. Sea salt adhesion amount in comparison to the original bridge for the case with noise barriers installed at the leading and trailing edges of the bridge deck, as shown in Figure 11

京都大学 KYOTO UNIVERSITY
A Self-archived copy in
Kyoto University Research Information Repository
https://repository.kulib.kyoto-u.ac.jp
京都大学学術情報リポジトリ KURENAI 紅 Kyoto University Research Information Repository

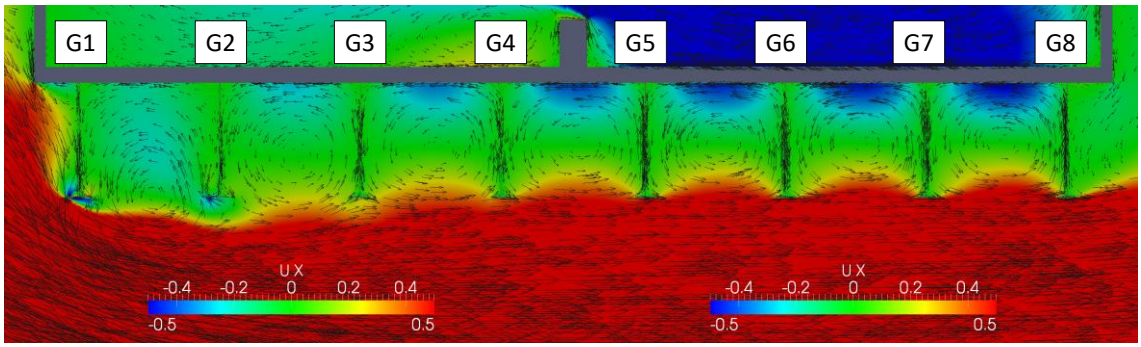

Figure 13. Contour diagram of time averaged wind velocity (m/s) for the case with noise barriers installed above the bridge deck, as shown in Figure 11, with H_L = 5 m, H_C = 1 m, and H_T = 5 m

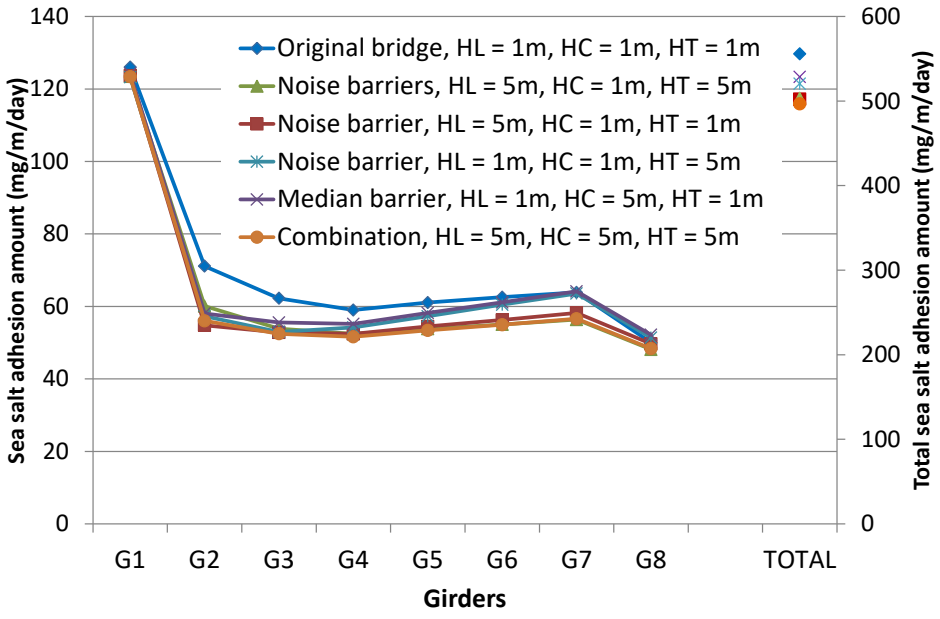

Figure 14. Sea salt adhesion amount in comparison to the original bridge for the case with noise barriers, median barrier, and a combination of both installed above the bridge deck, as shown in Figure 11

京都大学 KYOTO UNIVERSITY
A Self-archived copy in
Kyoto University Research Information Repository
https://repository.kulib.kyoto-u.ac.jp
京都大学学術情報リポジトリ KURENAI 紅 Kyoto University Research Information Repository

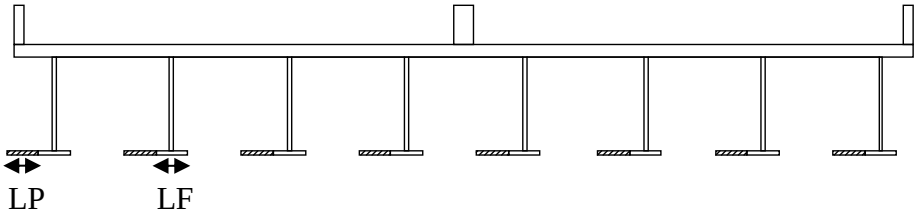

Figure 15. Illustration of horizontal plates installed on the bridge girders oriented towards the upstream direction with LP = LF (Case H1)

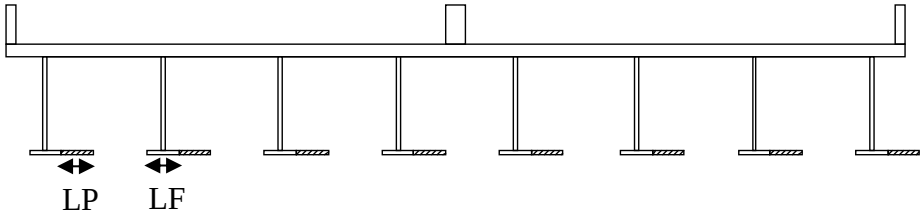

Figure 16. Illustration of horizontal plates installed on the bridge girders oriented towards the downstream direction with LP = LF (Case H2)

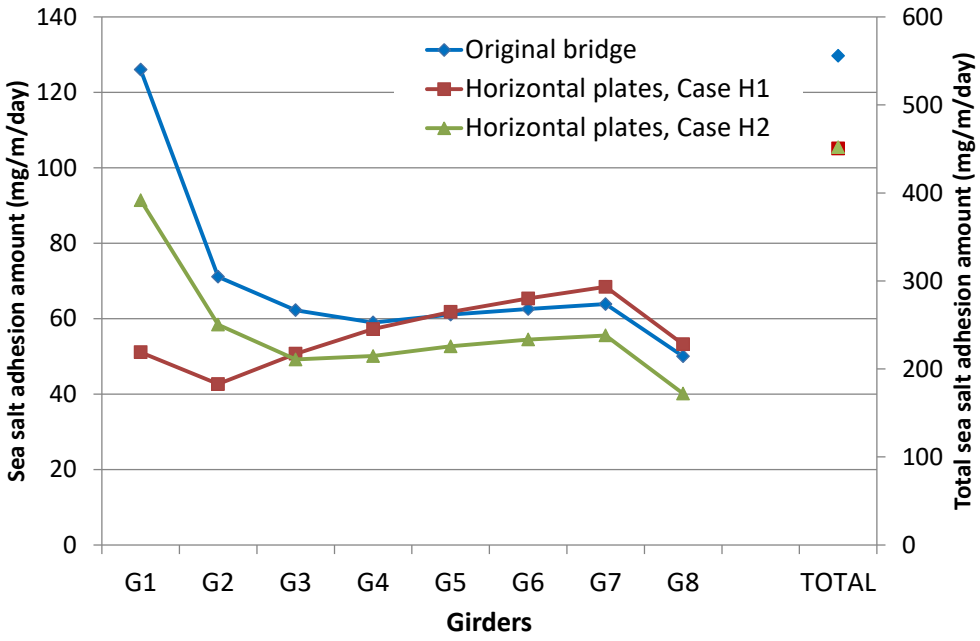

Figure 17. Sea salt adhesion amount in comparison to the original bridge for the case with horizontal plates installed on the bridge girders illustrated by Case H1 in Figure 16 and Case H2 in Figure 17

京都大学 KYOTO UNIVERSITY
A Self-archived copy in
Kyoto University Research Information Repository
https://repository.kulib.kyoto-u.ac.jp
京都大学学術情報リポジトリ KURENAI 紅 Kyoto University Research Information Repository

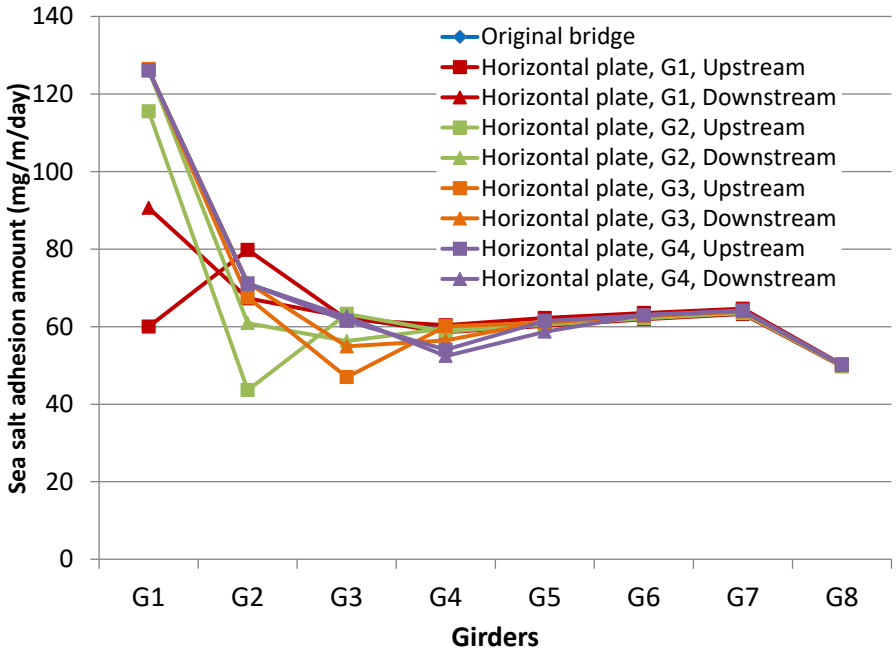

(a)

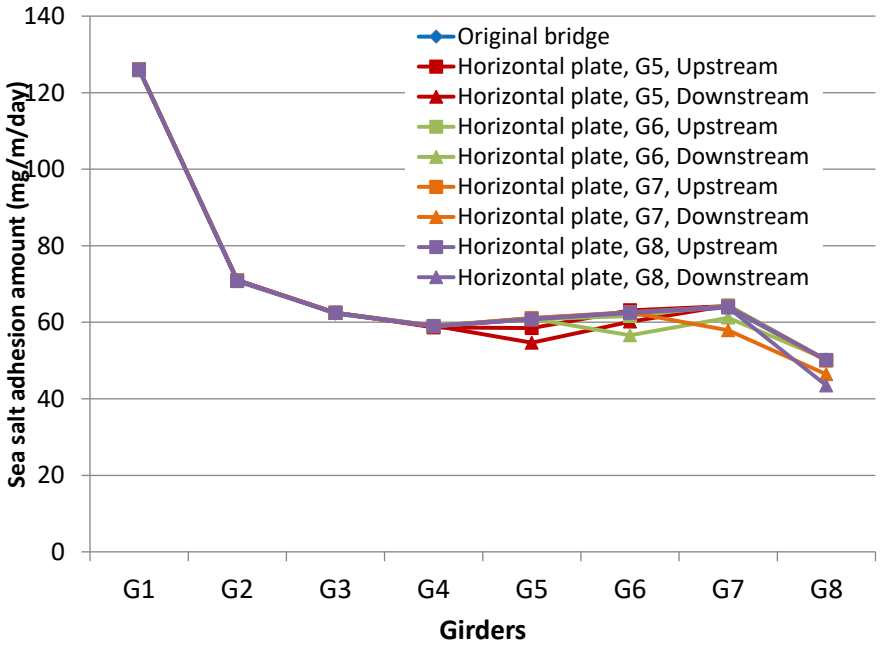

(b)

Figure18. Sea salt adhesion amount in comparison to original bridge for the case with a single horizontal plate installed on each girder at a time oriented towards the upstream and downstream directions with LP = LF

京都大学 KYOTO UNIVERSITY
A Self-archived copy in
Kyoto University Research Information Repository
https://repository.kulib.kyoto-u.ac.jp
京都大学学術情報リポジトリ KURENAI 紅 Kyoto University Research Information Repository

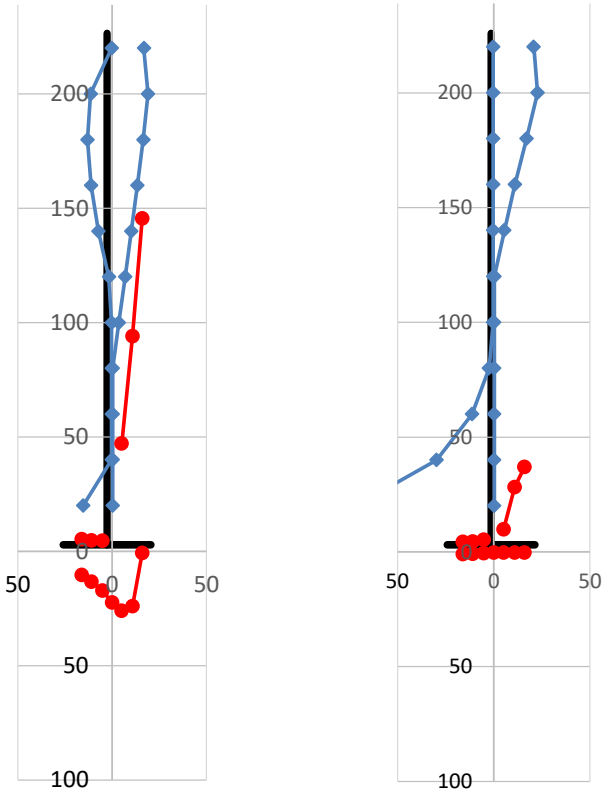

G1, upstream G5, downstream

Figure 19. Distribution of sea salt adhesion amount (mg/m^2/day) for a single horizontal plate installed on the bridge oriented towards the upstream on G1 and downstream on G5

京都大学 KYOTO UNIVERSITY
A Self-archived copy in
Kyoto University Research Information Repository
https://repository.kulib.kyoto-u.ac.jp
京都大学学術情報リポジトリ KURENAI 紅 Kyoto University Research Information Repository

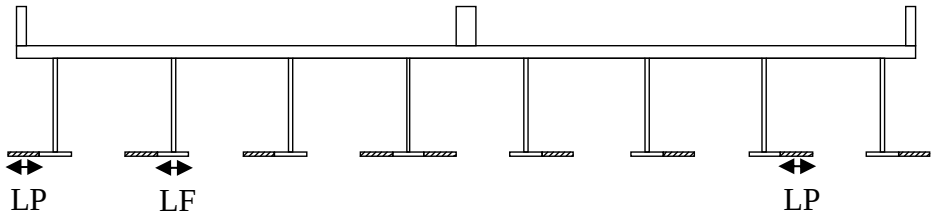

Figure 20. Illustration of horizontal plates installed oriented towards the upstream on the upstream side of the bridge and downstream on the downstream side of the bridge with LP = LF (Case H3)

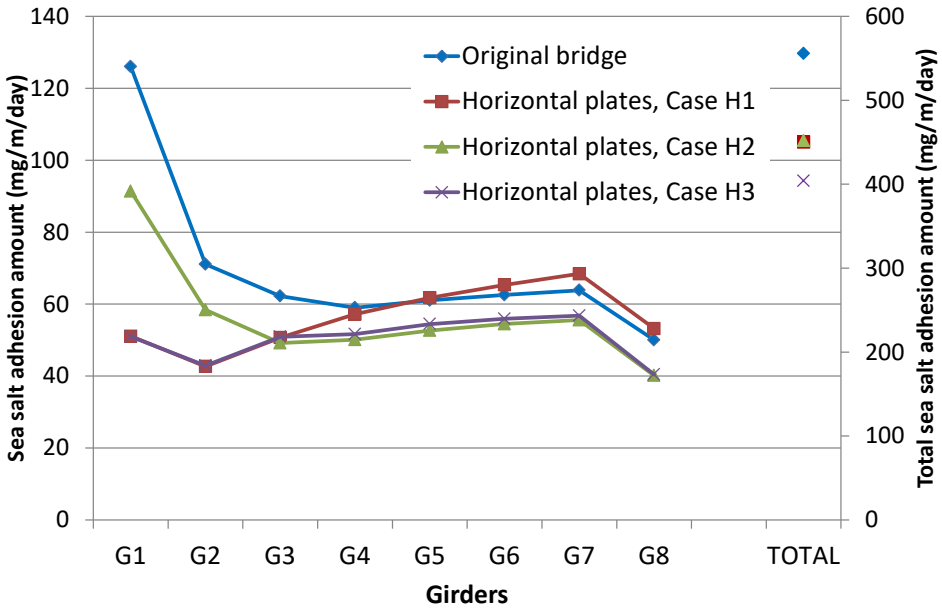

Figure 21. Sea salt adhesion amount in comparison to the original bridge for the case with horizontal plates installed on the bridge girders illustrated by Case H1 in Figure 15, Case H2 in Figure 16, and Case H3 in Figure 20

京都大学 KYOTO UNIVERSITY
A Self-archived copy in
Kyoto University Research Information Repository
https://repository.kulib.kyoto-u.ac.jp
京都大学学術情報リポジトリ KURENAI 紅 Kyoto University Research Information Repository

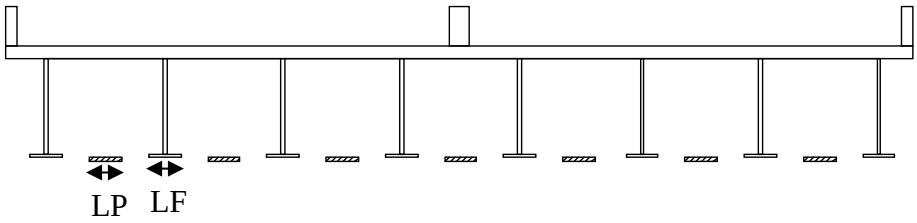

Figure 22. Illustration of horizontal plates installed between the bridge girders with LP = LF (Case H4)

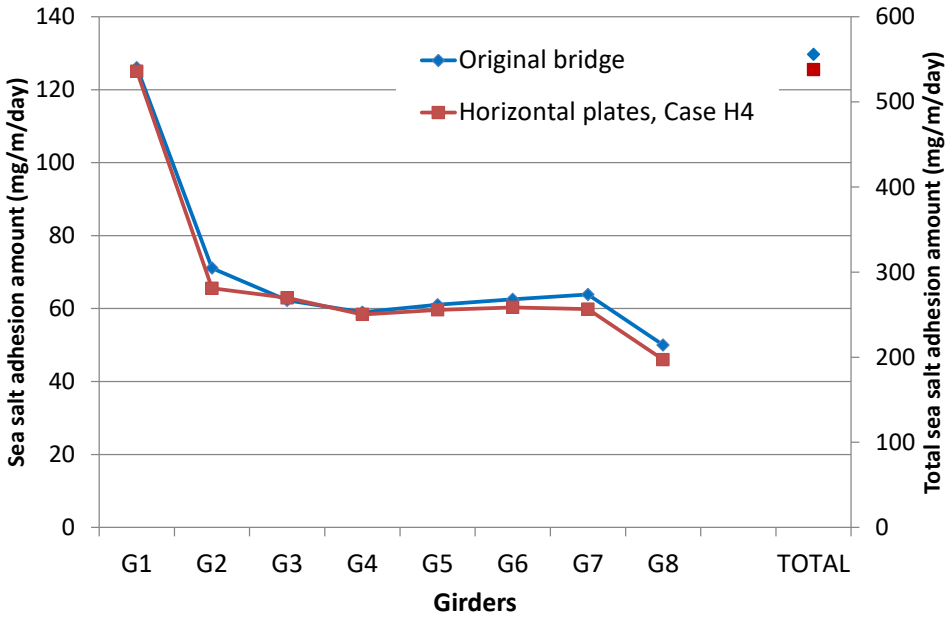

Figure 23. Sea salt adhesion amount in comparison to the original bridge for the case with horizontal plates installed between bridge girders illustrated by Case H4 in Figure 22

京都大学 KYOTO UNIVERSITY
A Self-archived copy in
Kyoto University Research Information Repository
https://repository.kulib.kyoto-u.ac.jp
京都大学学術情報リポジトリ KURENAI 紅 Kyoto University Research Information Repository

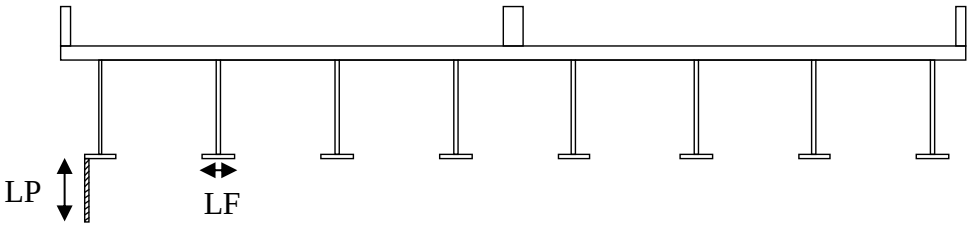

Figure 24. Illustration of a vertical plate installed on the most upstream girder (Case V1)

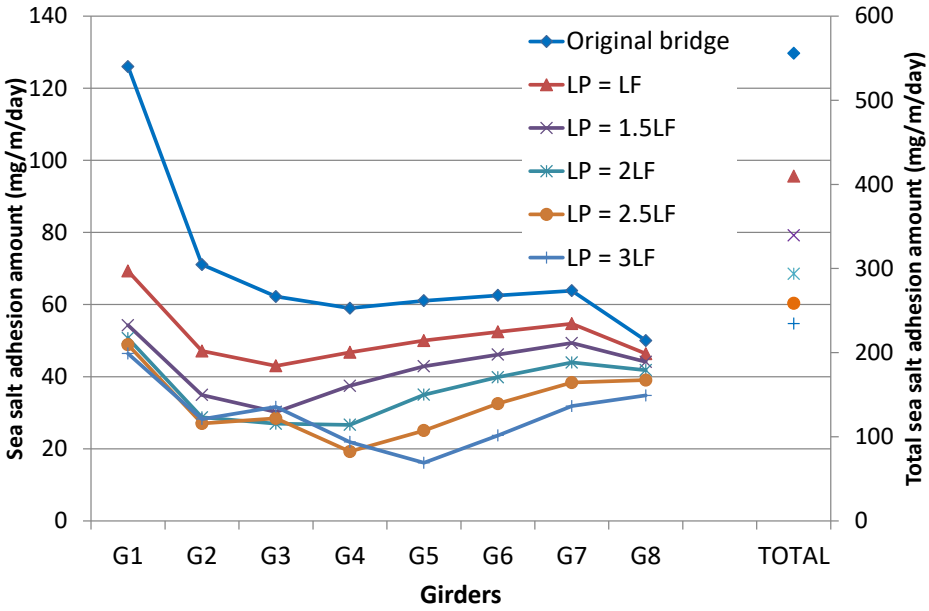

Figure 25. Sea salt adhesion amount in comparison to the original bridge for the case with a vertical plate installed on the most upstream girder illustrated by Case V1 in Figure 24

京都大学 KYOTO UNIVERSITY
A Self-archived copy in
Kyoto University Research Information Repository
https://repository.kulib.kyoto-u.ac.jp
京都大学学術情報リポジトリ KURENAI 紅 Kyoto University Research Information Repository

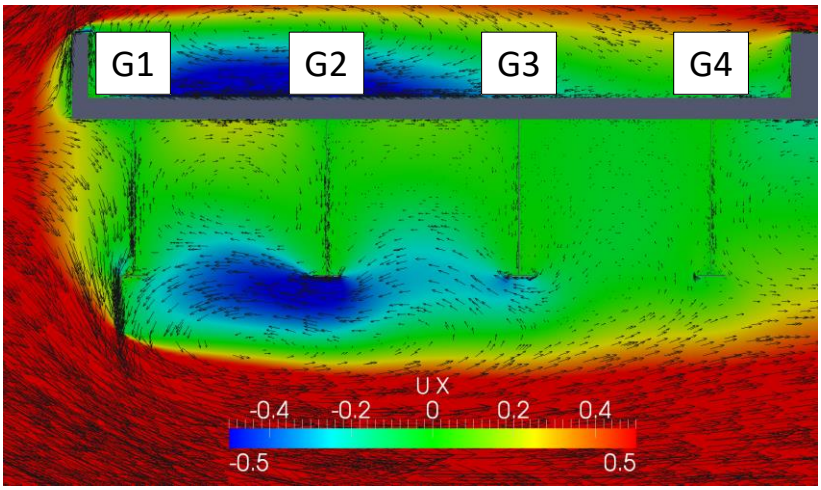

Figure 26. Contour diagram of time averaged wind velocity (m/s) on the upstream side of the bridge for a vertical plate installed on the most upstream girder illustrated by Case V1 in Figure 24 with LP = 2LF

京都大学 KYOTO UNIVERSITY
A Self-archived copy in
Kyoto University Research Information Repository
https://repository.kulib.kyoto-u.ac.jp
京都大学学術情報リポジトリ KURENAI 紅 Kyoto University Research Information Repository

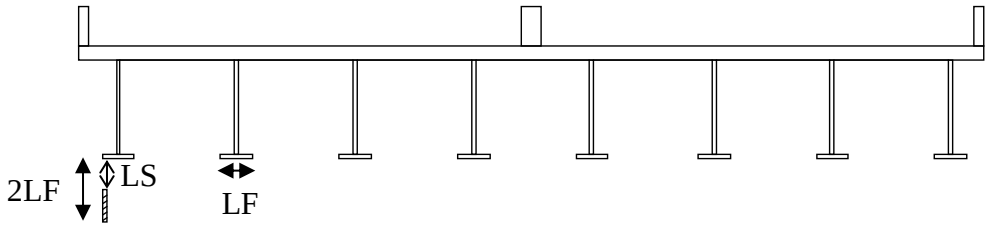

Figure 27. Illustration of a vertical plate with a slit of length LS installed on the most upstream girder (Case V2)

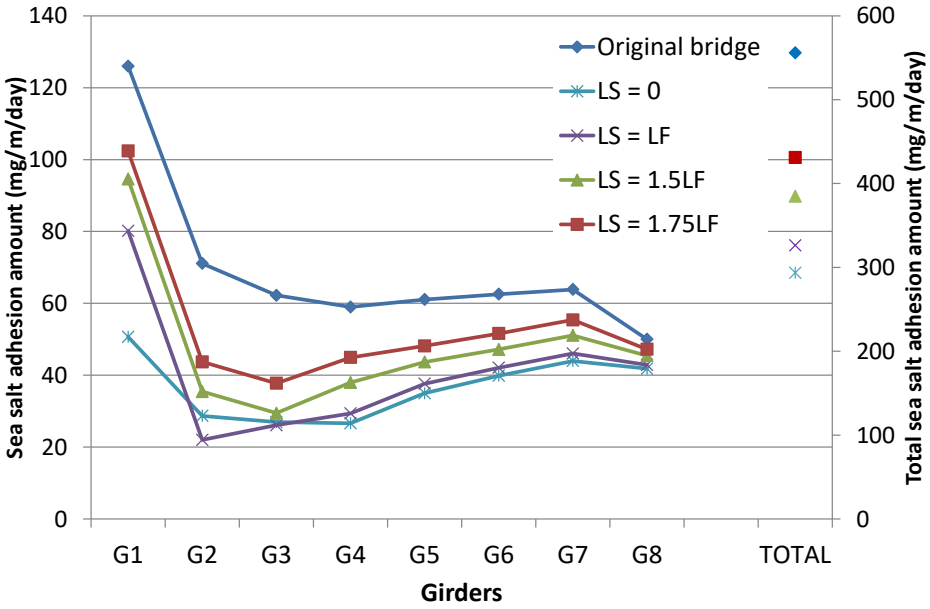

Figure 28. Sea salt adhesion amount in comparison to the original bridge for the case with a vertical plate with a slit installed on the most upstream girder illustrated by Case V2 in Figure 27

京都大学 KYOTO UNIVERSITY
A Self-archived copy in
Kyoto University Research Information Repository
https://repository.kulib.kyoto-u.ac.jp
京都大学学術情報リポジトリ KURENAI 紅 Kyoto University Research Information Repository

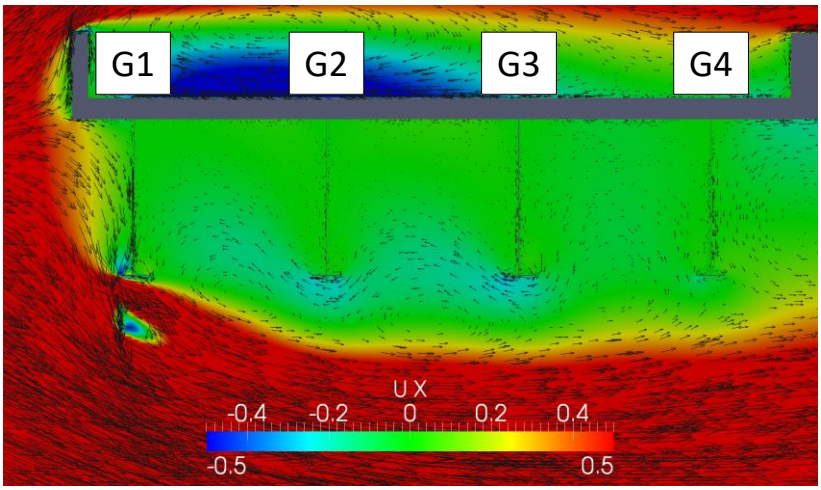

Figure 29. Contour diagram of time averaged wind velocity (m/s) on the upstream side of the bridge for a vertical plate with a slit installed on the most upstream girder illustrated by Case V2 in Figure 27 with LS = LF

京都大学 KYOTO UNIVERSITY
A Self-archived copy in
Kyoto University Research Information Repository
https://repository.kulib.kyoto-u.ac.jp
京都大学学術情報リポジトリ KURENAI 紅 Kyoto University Research Information Repository

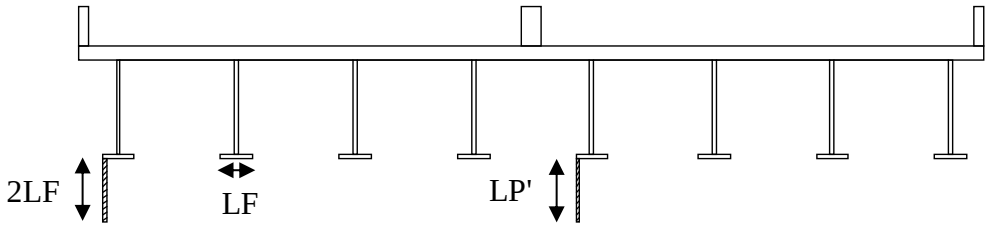

Figure 30. Illustration of an additional vertical plate for second phase flow separation installed on G5 (Case V3)

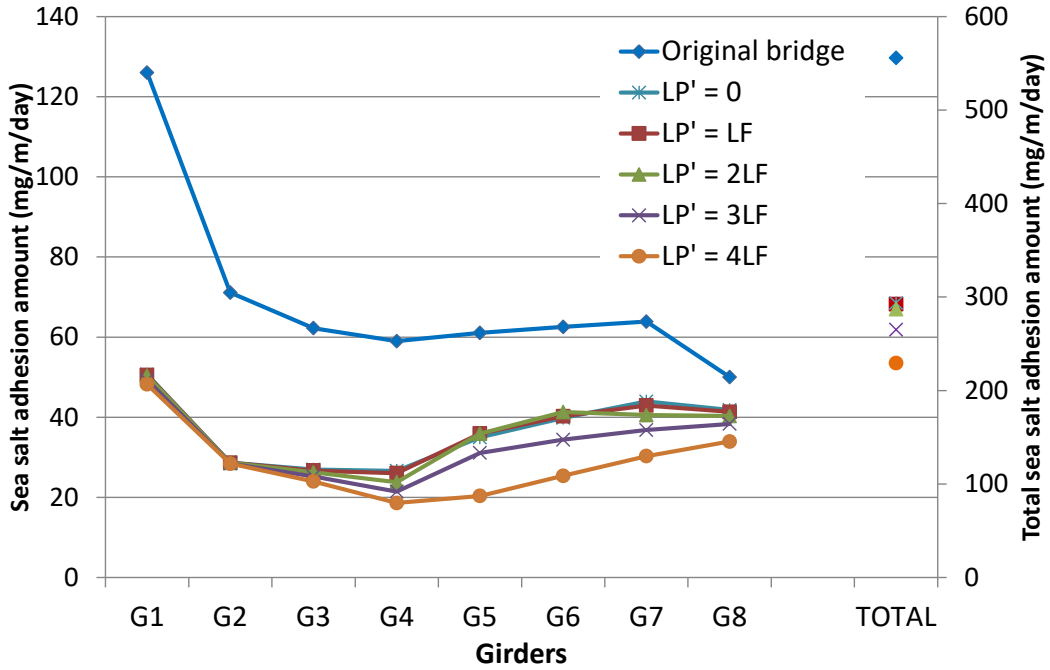

Figure 31. Sea salt adhesion amount in comparison to the original bridge for the case with an additional vertical plate for second phase flow separation installed on the downstream side of the bridge illustrated by Case V3 in Figure 30

A Self-archived copy in
Kyoto University Research Information Repository
https://repository.kulib.kyoto-u.ac.jp

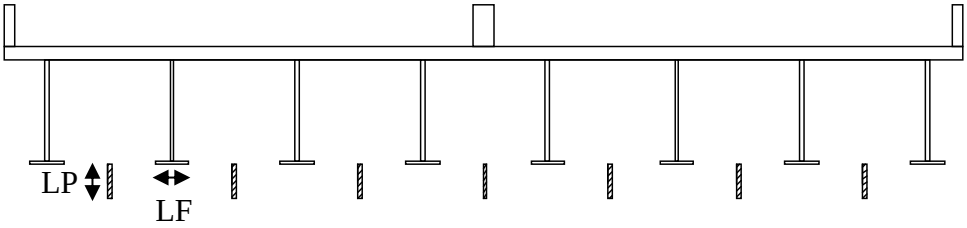

Figure 32. Illustration of vertical plates installed between the bridge girders (Case V4)

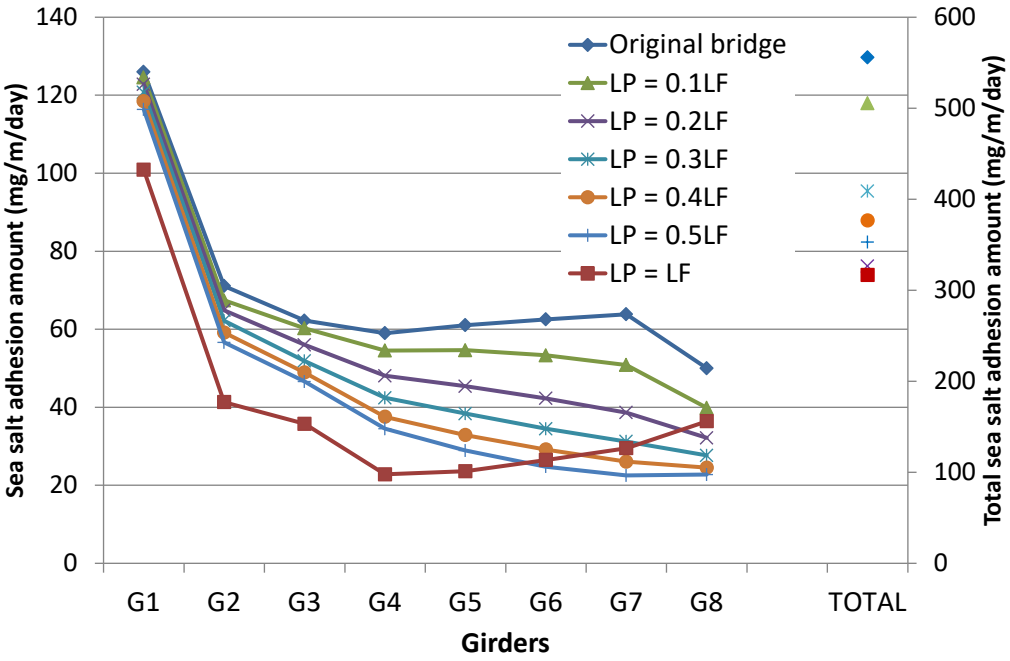

Figure 33. Sea salt adhesion amount in comparison to the original bridge for the case with vertical plates installed between bridge girders illustrated by Case V4 in Figure 32

A Self-archived copy in
Kyoto University Research Information Repository
https://repository.kulib.kyoto-u.ac.jp

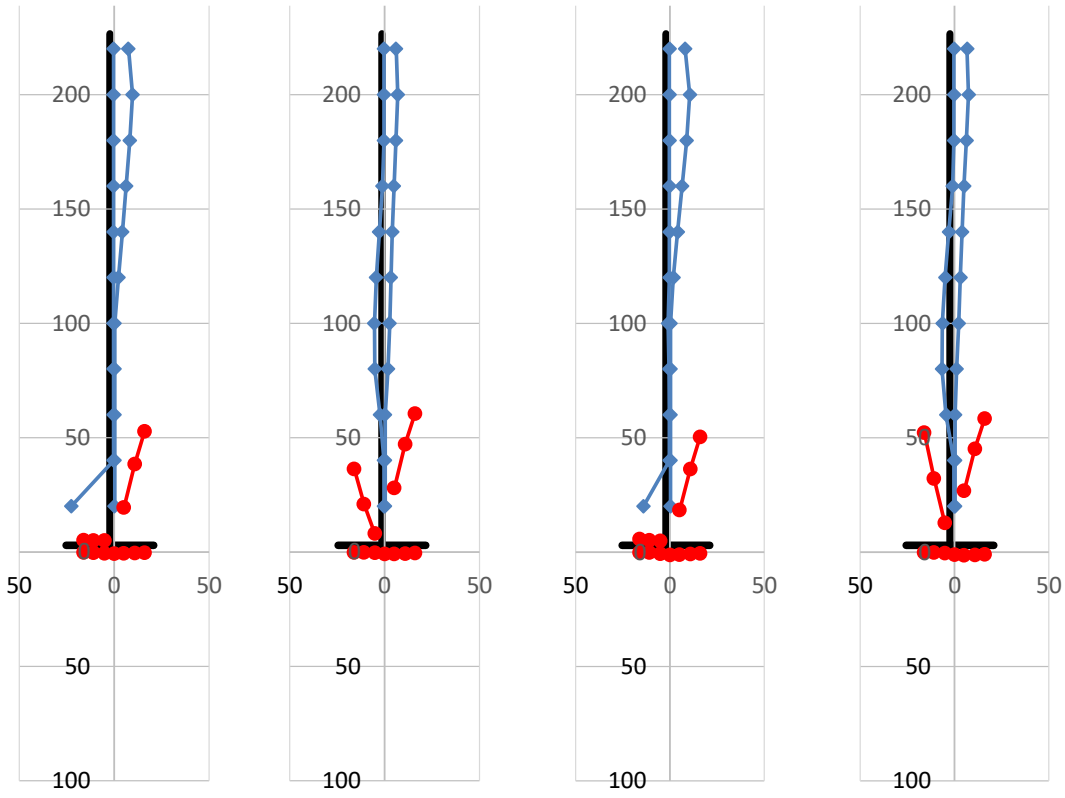

Figure 34. Comparison of sea salt adhesion amount distribution (mg/m^2/day) on G6 and G7 for vertical plates installed between the bridge girders illustrated by Case V4 in Figure 32

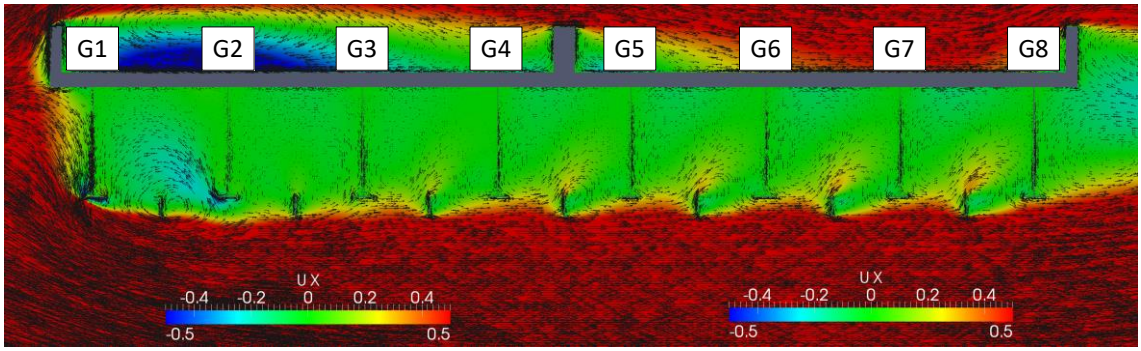

Figure 35. Contour diagram of time averaged wind velocity (m/s) for vertical plates installed between the bridge girders illustrated by Case V4 in Figure 32 with LP = LF

京都大学 KYOTO UNIVERSITY
A Self-archived copy in
Kyoto University Research Information Repository
https://repository.kulib.kyoto-u.ac.jp
京都大学学術情報リポジトリ KURENAI 紅 Kyoto University Research Information Repository

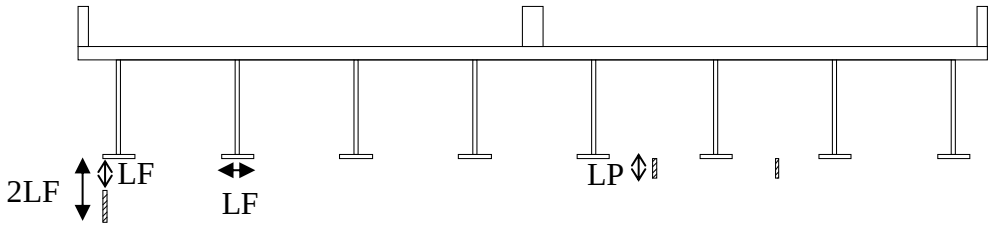

Figure 36. Illustration of a combination of a vertical plate with a slit installed on the most upstream girder with additional vertical plates installed between girders on the downstream side of the bridge (Case V5)

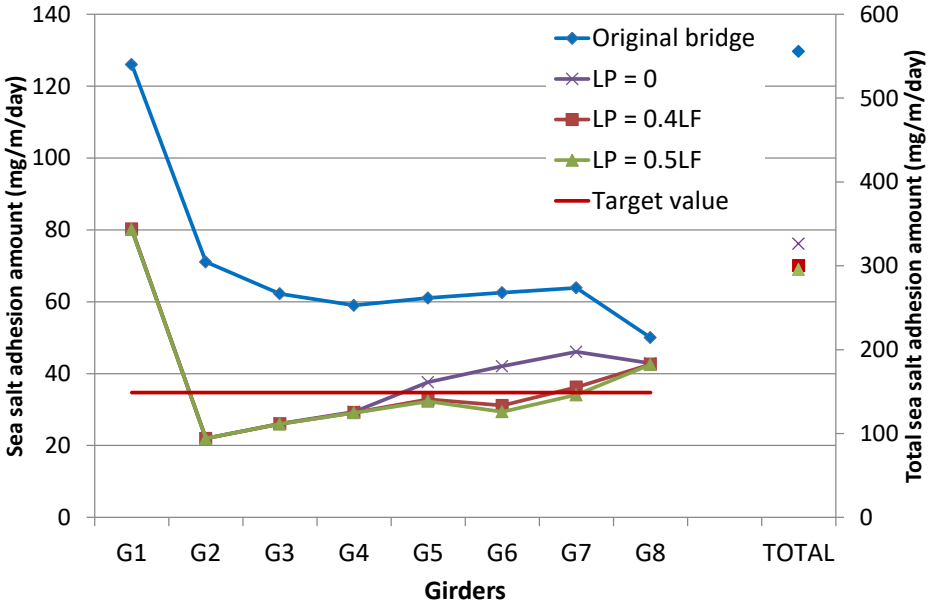

Figure 37. Sea salt adhesion amount in comparison to the original bridge for the case with a combination of vertical plates illustrated by Case V5 in Figure 36

A Self-archived copy in
Kyoto University Research Information Repository
https://repository.kulib.kyoto-u.ac.jp

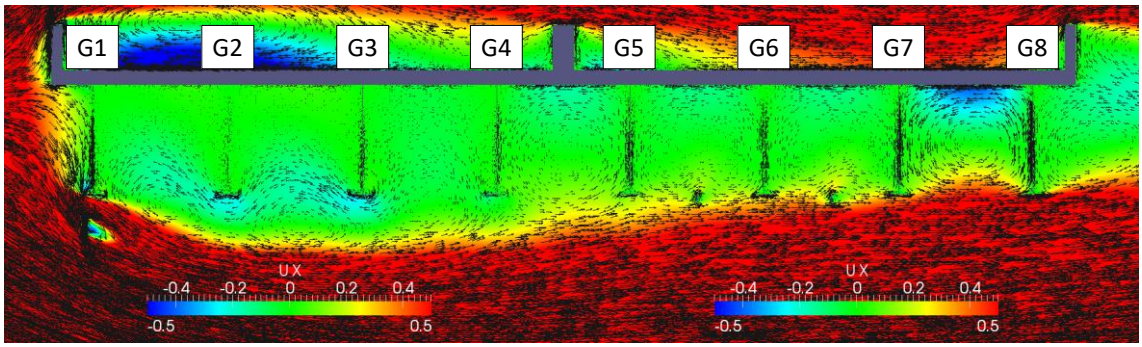

Figure 38. Contour diagram of time averaged wind velocity (m/s) for a combination of a vertical plate with a slit installed on the most upstream girder with additional vertical plates installed between girders on the downstream side of the bridge illustrated by Case V5 in Figure 36 with LP = 0.5LF

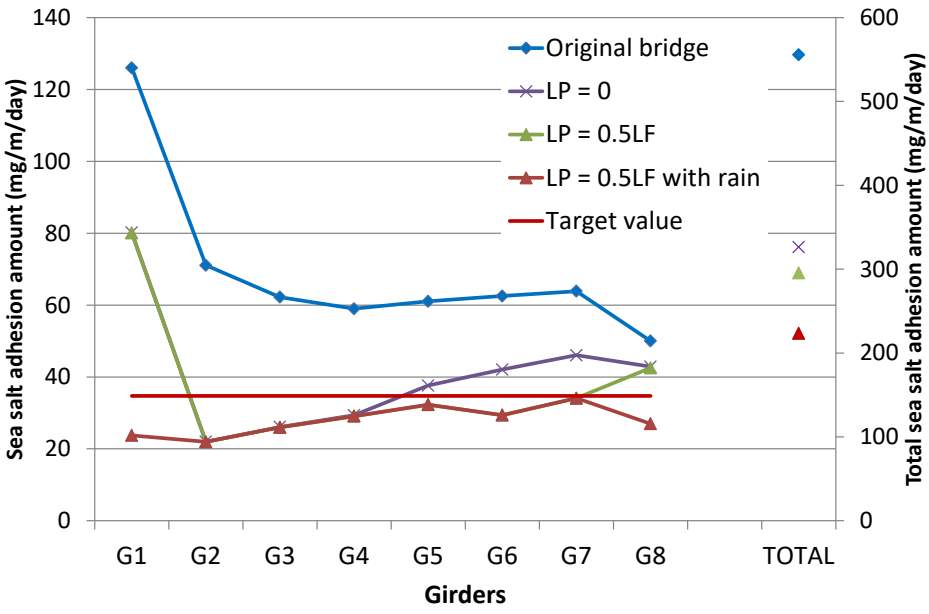

Figure 39. Sea salt adhesion amount after application of the washing-out effect due to rain to the results shown in Figure 37